Heme Binding Properties of Glyceraldehyde-3-phosphate Dehydrogenase

ARTICLE *in* BIOCHEMISTRY · SEPTEMBER 2012

Impact Factor: 3.02 · DOI: 10.1021/bi300863a · Source: PubMed

BIOCHEMISTRY
including biophysical chemistry & molecular biology

Article

pubs.acs.org/biochemistry

Heme Binding Properties of Glyceraldehyde-3-phosphate Dehydrogenase

Luciana Hannibal,[†] Daniel Collins,[‡] Julie Brassard,[∥] Ritu Chakravarti,[†] Rajesh Vempati,[†] Pierre Dorlet,[§] Jérôme Santolini,[§] John H. Dawson,[‡] and Dennis J. Stuehr*,[†]

[†]Department of Pathobiology, Lerner Research Institute, Cleveland Clinic, Cleveland, Ohio 44195, United States

[‡]Department of Chemistry and Biochemistry, University of South Carolina, Columbia, South Carolina 29208, United States

[§]Laboratoire Stress Oxydant et Détoxication (LSOD), UMR 8221, CNRS-CEA-Univ Paris-Sud, Saclay, France

[∥]Agriculture and Agri-Food Canada, Food Research and Development Centre, 3600 Casavant West, Saint-Hyacinthe, Québec, Canada, J2S 8E3

Supporting Information

ABSTRACT: Glyceraldehyde-3-phosphate dehydrogenase (GAPDH) is a glycolytic enzyme that also functions in transcriptional regulation, oxidative stress, vesicular trafficking, and apoptosis. Because GAPDH is required for the insertion of cellular heme into inducible nitric oxide synthase [Chakravarti, R., et al. (2010) *Proc. Natl. Acad. Sci. U.S.A. 107*, 18004−18009], we extensively characterized the heme binding properties of GAPDH. Substoichiometric amounts of ferric heme bound to GAPDH (one heme per GAPDH tetramer) to form a low-spin complex with UV−visible maxima at 362, 418, and 537 nm and when reduced to ferrous gave maxima at 424, 527, and 559 nm. Ferric heme association and dissociation rate constants at 10 °C were as follows: k_{on} = 17800 M^{-1} s^{-1}, k_{off1} = 7.0 × 10^{-3} s^{-1}, and k_{off2} = 3.3 × 10^{-4} s^{-1} (giving approximate affinities of 19−390 nM). Ferrous heme bound more poorly to GAPDH and dissociated with a k_{off} of 4.2 × 10^{-3} s^{-1}. Magnetic circular dichroism, resonance Raman, and electron paramagnetic resonance spectroscopic data on the ferric, ferrous, and ferrous−CO complexes of GAPDH showed that the heme is bis-ligated with His as the proximal ligand. The distal ligand in the ferric complex was not displaced by CN^- or N_3^- but in the ferrous complex could be displaced by CO at a rate of 1.75 s^{-1} (for >0.2 mM CO). Studies with heme analogues revealed selectivity toward the coordinating metal and porphyrin ring structure. The GAPDH−heme complex was isolated from bacteria induced to express rabbit GAPDH in the presence of δ-aminolevulinic acid. Our finding of heme binding to GAPDH expands the protein's potential roles. The strength, selectivity, reversibility, and redox sensitivity of heme binding to GAPDH are consistent with it performing heme sensing or heme chaperone-like functions in cells.

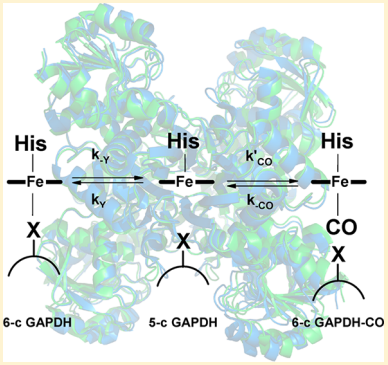

Glyceraldehyde-3-phosphate dehydrogenase (GAPDH, EC 1.2.1.12) catalyzes the conversion of glyceraldehyde 3-phosphate into glycerate 1,3-bisphosphate. Besides its housekeeping role in the glycolytic pathway,[4] eukaryotic GAPDHs participate in an array of cellular functions, including transcription, oxidative stress, apoptosis, and autophagy.[5,6] A great deal of this functional diversity is attained via changes in the subcellular localization and/or posttranslational modifications. GAPDHs are widely distributed in Nature, ranging from bacteria and Archaea to animals, including humans.[7] Prokaryotic GAPDHs are similarly versatile; some of their functions include binding to mammalian proteins, receptor-mediated acquisition of transferrin-bound iron, ADP ribosylation, and prokaryotic−eukaryotic cell−cell communication.[8]

Since its original isolation from rabbit muscle in 1964 by W. Ferdinand,[9] research on the functional versatility of GAPDH has mounted steadily. A perhaps underappreciated feature of GAPDH concerns its reported yet unexplored interactions with heme[10−12] and the recently proposed role of heme in the regulation of the protein's expression in red blood cells.[13] Our laboratory has recently shown that GAPDH is required for heme transfer into the apo form of inducible NO synthase and that this process is regulated by the protein's ability to undergo S-nitrosylation.[14]

The superfamily of canonical (the term "canonical" refers to proteins with a defined heme binding site that is highly conserved across species) heme proteins includes globins, cytochromes, cytochrome P450 monooxygenases, nitric oxide synthases, heme oxygenases, guanylate cyclases, catalases, and peroxidases. These proteins accomplish a wide range of functions, including oxygen transport, electron transfer, gaseous molecule sensing, and heme degradation. The heme binding site in each member of this superfamily is highly conserved across species. The recent years have witnessed the identification of a number of noncanonical heme binding proteins. These proteins present nonstandard heme binding

Received: June 27, 2012
Revised: September 6, 2012
Published: September 7, 2012

dx.doi.org/10.1021/bi300863a | *Biochemistry* 2012, 51, 8514−8529

sites[15,16] and usually bind the cofactor in a reversible fashion, and in some cases, their function requires the switching of the axial ligands coordinating the heme moiety.[17−19] Noncanonical heme binding proteins participate in diverse functions, including heme trafficking, intracellular signaling, and the regulation of gene expression.

One major experimental setback in identifying the proteins involved in heme metabolism has been the inability to isolate cellular synthesis and degradation of heme from the intracellular trafficking events.[20] We proposed that GAPDH may participate in the regulation of heme metabolism by controlling the insertion of heme into apoproteins.[14] However, the biophysical characteristics of the binding of heme to GAPDH remain unexplored. Here, we set out to investigate the details of the novel interaction between GAPDH and Fe(III)-protoporphyrin IX. We found that GAPDH binds heme to form a complex with spectral features that are reminiscent of certain *b*-type cytochromes and other heme binding proteins featuring bis-His axial ligation. Binding of heme by GAPDH is a reversible and redox-sensitive process and in general is reminiscent of noncanonical heme binding proteins involved in heme sensing and transport.

MATERIALS AND METHODS

Reagents. Rabbit muscle GAPDH (rGAPDH) and human erythrocyte GAPDH (hGAPDH) were purchased from Sigma (St. Louis, MO). Hemin chloride was purchased from MP Biomedicals (Solon, OH). CO gas was obtained from Praxair, Inc. (Danbury, CT). EPPS was purchased from Fisher Scientific (Pittsburgh, PA). DTT was purchased from RPI Corp. (Mount Prospect, IL). All other reagents were purchased from Sigma. Apomyoglobin (expression plasmid kindly provided by J. Olson) was produced in-house according to a published procedure.[21]

Protein Expression and Purification. The wild-type rabbit GAPDH gene was synthesized by Genscript with codon optimization for optimal expression in *Escherichia coli*, according to the cDNA sequence reported in the NCBI database [GI:160332366 (http://www.uniprot.org/uniprot/P46406)]. Wild-type and mutant rabbit GAPDH (rrGAPDH) coding sequences were subcloned into the pET15b vector using the NdeI and XhoI restriction sites. The resulting rrGAPDH constructs containing a His_6 tag attached to their N-termini were overexpressed in *E. coli* strain BL21(DE3). All the proteins were expressed and purified according to standard procedures. Briefly, 25 mL of an overnight Luria broth culture of *E. coli* carrying the construct of interest was added to 0.5 L of terrific broth supplemented with 125 μg/mL ampicillin. Cells were induced with 1 mM IPTG after the optical density had reached 0.8−1.0, followed by additional growth for 48 h at room temperature. When appropriate, TB cultures were supplemented with 0.5 mM δ-aminolevulinic acid (heme biosynthesis precursor) at the time of induction to isolate heme-bound rabbit, human, or *Streptococcus suis* GAPDHs. Purification of wild-type and variant rrGAPDH was performed by lysis and sonication followed by Ni-NTA affinity chromatography according to the manufacturer's instructions (Amersham Biosciences). Digestion with thrombin yielded 85% His_6-free rrGAPDH. The purity of the final preparations (90−95% rrGAPDH) was assessed by sodium dodecyl sulfate−polyacrylamide gel electrophoresis (SDS−PAGE). The UV−visible and kinetic properties (k_{on} and k_{off} for heme) of commercial and recombinant rabbit GAPDHs were identical; hence, commercial rGAPDH was utilized for all studies not requiring in vivo expression and reconstitution with heme.

Human recombinant GAPDH (hrGAPDH) was expressed as a GST fusion protein according to a published procedure.[22] When appropriate, cultures were supplied with 0.5 mM δ-aminolevulinic acid (heme biosynthesis precursor) at the time of induction to isolate heme-bound hrGAPDH. All the heme binding studies presented herein were performed with pure hrGAPDH obtained upon digestion of GST-bound hrGAPDH with thrombin followed by purification on a GSH resin according to the manufacturer's instructions (Novagen).

S. suis. GAPDH-His_6 was expressed according to a published procedure.[23] Purification of the His_6-tagged protein was conducted using Ni-NTA affinity chromatography as described for rrGAPDH.

Analytical Gel Filtration. The oligomeric state and the stability of binding of heme to GAPDH were assessed by analytical gel filtration. Protein samples (~300 μM) in EPPS buffer (40 mM, pH 7.6, 150 mM NaCl) were incubated with 30 μM hemin for 1 h at 4 °C. Samples of apo-GAPDH or GAPDH−heme complexes were injected on a Superdex 200 resin pre-equilibrated with EPPS buffer (40 mM, pH 7.6, 150 mM NaCl).

Activity Assays. GAPDH activity was measured by the method of Ferdinand.[9] The assay solution contained triethanolamine (40 mM), Na_2HPO_4 (50 mM), 0.2 mM EDTA (pH 8.9), 2 mM NAD, and 2 mM D-glyceraldehyde 3-phosphate. The reaction was started by the addition of ~1 μg of enzyme. The reaction was followed at 340 nm (formation of NADH; ε_{340} = 6.22 mM^{-1} cm^{-1}).

Heme Staining Assay. The retention of heme by wild-type and variant GAPDH was assessed by in-gel heme staining according to the modified procedure of Guo et al.[24] Apo and heme-loaded GAPDH (~30 μg) were examined for their ability to retain heme under nonreducing 10% SDS−PAGE conditions.

Redox Titrations. Spectroelectrochemical titrations were conducted in a glovebox (Belle Technology, Dorset, U.K.) under a N_2 atmosphere as previously described.[25] Briefly, GAPDH−heme samples were made anaerobic by gel filtration in a Sephadex G-25 column (PD 10, GE Healthcare) equilibrated with anaerobic buffer [100 mM phosphate buffer (pH 7.0) and 125 mM NaCl]. Protein samples were diluted to a final volume of 3.5 mL (final concentration of ≈10 μM), and the following electron mediator dyes (0.5−1 μM) were used: potassium ferricyanide (E_m = 450 mV), quinhydrone (E_m = 280 mV), dichlorophenolindophenol (E_m = 217 mV), phenazine methosulfate (E_m = 80 mV), 1,4-naphthoquinone (E_m = 60 mV), 2-hydroxy-1,4-naphthoquinone (E_m = −137 mV), anthraquinone 2-sulfonate (E_m = −225 mV), phenosafranine (E_m = −252 mV), benzyl viologen (E_m = −358 mV), and methyl viologen (E_m = −450 mV). The titration was conducted at 15 °C by bolus additions of potassium ferricyanide (oxidative titrations) or sodium dithionite (reductive titration). Absorption spectra were recorded with a Cary 50 spectrophotometer equipped with a dip-probe detector, and the potentials were measured with an Accumet AB15 pH meter (Fisher Scientific) using a silver/silver chloride microelectrode saturated with 4 M KCl.

UV−Visible Spectroscopy. UV−visible spectra of GAPDH, hemin (or hemin analogues), and GAPDH−hemin complexes were generated from freshly prepared samples of GAPDH and hemin. Hemin (or hemin analogue) stock

dx.doi.org/10.1021/bi300863a | *Biochemistry* 2012, 51, 8514−8529

solutions (2.5 mM) were prepared by dissolving solid hemin in 0.1 M NaOH and 5% dimethyl sulfoxide. The latter was included to prevent the formation of heme dimers.[17,26] The concentration of hemin was calculated on the basis of the ε_{385} of 58.4 mM^{-1} cm^{-1} [27] or by means of the pyridine hemochrome method.[28,29] The concentration of heme-free GAPDH was determined using an absorption coefficient of 30.4 mM^{-1} cm^{-1} at 280 nm. Typically, ferrous GAPDH−heme complexes were generated by the addition of a slight excess of dithionite. Ferrous−CO complexes were generated by direct bubbling of CO into a prereduced GAPDH−heme complex.

Ethoxylation of His Residues with Diethyl Pyrocarbonate (DEPC). Two hundred microliters of 100 μM rGAPDH or preformed rGAPDH−heme complex (100 μM rGAPDH and 20 μM heme) was incubated with 15 mM DEPC (44 μL of a 68 mM freshly prepared stock solution of DEPC) for 2 °C on ice. The reactions were performed in 40 mM EPPS (pH 7.6) supplemented with 150 mM NaCl and 10% glycerol. Three rounds of buffer exchange were then applied using 0.5 mL microcentrifuge spin columns with a molecular mass cutoff of 10 kDa. The concentrated samples (~100 μL) were diluted to 500 μL with the same buffer (final protein concentration of ~40 μM) and the spectra recorded before and after the addition of 8 μM freshly prepared hemin (1.5 μL of a 2.4 mM stock).

Resonance Raman Spectroscopy. Samples (50 μL) of ferric, ferrous, or ferrous GAPDH−CO solutions at 70−150 μM were prepared in gastight quartz EPR tubes and disposed in a homemade spinning cell, at room temperature, to avoid local heating and to prevent photodissociation and degradation. Raman excitation at 413.1 nm was achieved with a laser power of ~10 mW. Resonance Raman spectra were recorded using a modified single-stage spectrometer (Jobin-Yvon T64000, HORIBA Jobin Yvon S.A.S., Chilly Mazarin, France) equipped with a liquid N_2-cooled back-thinned CCD detector. Stray scattered light was rejected using a holographic notch filter (Kaiser Optical Systems, Ann Arbor, MI). Spectra correspond to the average of three different 1 h accumulations. Neutral density filters were used for the ferrous−CO complexes to decrease the laser power (below 5 mW at the sample) and prevent photodissociation and photo-oxidation. The spectral accuracy was estimated to be ±1 cm^{-1}. The spectral resolution was ~3 cm^{-1}. Baseline correction was performed using GRAMS 32 (Galactic Industries, Salem, NH).

EPR Spectroscopy. X-Band (9.4 GHz) EPR spectra were recorded on a Bruker ELEXSYS 500 spectrometer equipped with a standard TE cavity (Bruker) and an Oxford Instruments continuous flow liquid helium cryostat interfaced with a temperature control system. Simulations were performed using the Easyspin software package.[30]

Magnetic Circular Dichroism. MCD spectra were measured with a magnetic field strength of 1.41 T by using a JASCO J815 spectropolarimeter. This instrument was equipped with a JASCO MCD-1B electromagnet and interfaced with a Silicon Solutions personal computer through a JASCO IF-815-2 interface unit. The acquisition and manipulation of data using Cary or Jasco software have been previously described.[31] Apo-rGAPDH was loaded with Fe(III) hemin to form the ferric complex. To ensure homogeneity, ferricyanide was used to fully oxidize the heme center, followed by desalting chromatography. The resulting spectra were compared to data from other proteins, and the most accurate match was with that of a bis-His(imidazole) coordinated heme center. Histidine is a common protein backbone heme axial ligand, so the data from Fe(III) rGAPDH were compared to those from two well-characterized ferric bis-His systems: cytochrome b_5 and the bis-imidazole-ligated H93G sperm whale myoglobin (Mb) mutant. Native ferric cytochrome b_5 has a six-coordinate, low-spin bis-His heme structure, and the H93G Mb system has two open axial pockets created by a mutation of the proximal ligand that allows for two exogenous ligands to bind to the heme; in this case, imidazole (Im) is used to create the same bis-His-type environment. All spectral measurements for the rGAPDH−heme complex were taken with a 0.2 cm quartz cuvette at 4 °C. Complete reduction of the heme iron was accomplished by adding a few microliters of a concentrated sodium dithionite solution (25 mg/mL of H_2O) with a microliter syringe. Ferrous−CO adducts were prepared by bubbling CO gas into the ferrous rGAPDH−heme samples. UV−visible absorption spectra were recorded with a Cary 400 spectrophotometer interfaced with a personal computer before and after the MCD measurements to verify sample integrity.

Binding Affinities. Spectrophotometric titrations were conducted by stepwise addition of 0−35 μM hemin to a sample of GAPDH (and to the protein-free buffer in the reference cuvette). Formation of the GAPDH−heme complex was characterized by a red shift in wavelength from 385 to 415 nm. Binding affinities (K_d) and stoichiometry were determined by plotting ΔA(415−700 nm) against the concentration of added hemin. The data were fit to the following equation:

$$A_{415} = \varepsilon_{415}\left\{[\text{hemin}] + K_d + \frac{A_{max}}{\varepsilon_{415}} - \left[\left([\text{hemin}] + K_d + \frac{A_{max}}{\varepsilon_{415}}\right)^2 - 4\left([\text{hemin}] + \frac{A_{max}}{\varepsilon_{415}}\right)\right]^{1/2}\right\}/2 \quad (1)$$

which accounts for the concentration of the protein present in the assay,[32] where [hemin] is the concentration of hemin added in the sample and reference cuvettes, ε_{415} is the absorption coefficient of the GAPDH-bound hemin (80 mM^{-1} cm^{-1}), and A_{max} is the absorbance of maximal binding.

Kinetics of Binding of Heme to GAPDH (k_{on}). Binding of heme to rGAPDH was examined by a stopped-flow method at 10 °C, using a Hi-Tech SF61-DX2 stopped-flow instrument (Hi-Tech Scientific, Salisbury, U.K.) coupled to a diode array detector. Briefly, 5 μM freshly prepared hemin was mixed with varying concentrations of rGAPDH (10−80 μM) in EPPS buffer (100 mM, pH 7.6) supplemented with 10% glycerol and 150 mM NaCl. Observed rate constants, k_{obs}, were calculated by fitting the data to a single-exponential equation.

Kinetics of Transfer of Heme from GAPDH to Apomyoglobin (k_{off}). The transfer of ferric heme from rGAPDH−heme complexes (10 μM GAPDH and 2 μM hemin) to apomyoglobin (50 μM) was measured by UV−vis spectrophotometry following the formation of holomyoglobin at 411 nm. GAPDH−heme complexes (5:1 molar ratio) were mixed with a 5-fold excess of apomyoglobin, and the reaction was allowed to proceed for 2 h. UV−vis spectra were recorded every 2 min. The transfer of ferrous heme to apomyoglobin was performed under the same conditions, except that protein samples and buffers were made anaerobic prior to the experiment. The reactions were conducted in a rubber septum-capped anaerobic cuvette. k_{off} rates were calculated by plotting the absorbance difference at 408 nm (absorption

dx.doi.org/10.1021/bi300863a | Biochemistry 2012, 51, 8514−8529

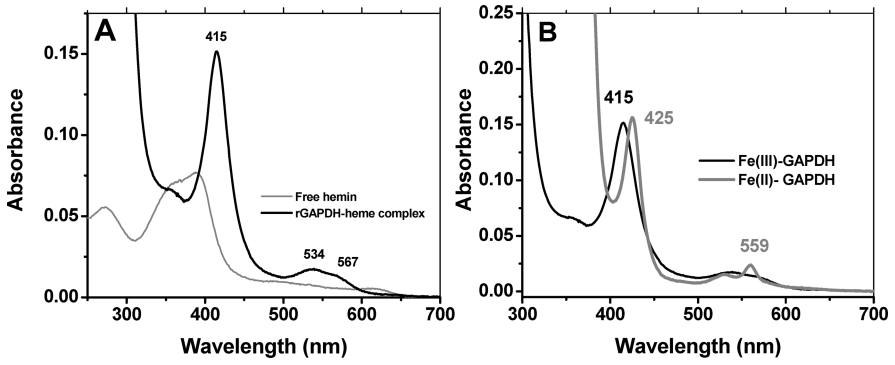

Figure 1. UV−vis spectrum of the rGAPDH-heme complex at pH 7.4. (A) UV−vis spectra of free hemin and hemin bound to rGAPDH. The ferric rGAPDH−heme complex is in a low-spin configuration. (B) UV−vis wavelength maxima of ferric and ferrous rGAPDH−heme complexes. Ferrous GAPDH displays absorption maxima at 425, 527, and 559 nm.

maximum for myoglobin) and 416 nm (absorption maximum for the GAPDH−heme complex) versus time.

Kinetics of Binding of CO to Fe(II) GAPDH. Rabbit GAPDH−heme complexes (5:1) were prepared by mixing freshly prepared GAPDH (40 μM) and hemin solutions (10 μM) in EPPS buffer (100 mM, pH 7.6) supplemented with 10% glycerol and 150 mM NaCl. The samples were made anaerobic, and ferrous GAPDH−heme complexes (Soret band appearing at 425 nm) were generated by adding a slight excess of dithionite. The samples were transferred to an anaerobic stopped-flow device using a gastight syringe and mixed with anaerobic buffer containing different concentrations of CO. Formation of the Fe(II)−CO−GAPDH complex was followed at 420 nm. Observed rate constants, k_{obs1} and k_{obs2}, were obtained by fitting the data to a two-exponential sequential model as the traces displayed a biphasic behavior.

Kinetics of Binding of NO to Fe(II) GAPDH. Rabbit GAPDH−heme complexes (5:1) were prepared by mixing freshly prepared GAPDH (final concentration of 100 μM) and hemin solutions (final concentration of 20 μM) in EPPS buffer (100 mM, pH 7.6) supplemented with 10% glycerol and 150 mM NaCl. The samples were made anaerobic, and the ferrous GAPDH−heme complex was generated by adding a slight excess of dithionite. The samples were transferred to an anaerobic stopped-flow device using a gastight syringe and mixed with anaerobic buffer containing different concentrations of NO. Formation of the Fe(II)−NO−GAPDH complex was followed at 424 nm (disappearance of the ferrous rGAPDH−heme complex) and 385 nm [formation of a Fe(II)−NO−rGAPDH complex]. Observed rate constants, k_{obs1} and k_{obs2}, were obtained by fitting the data to a two-exponential sequential model as the traces displayed a biphasic behavior.

RESULTS

Heme Binding to rGAPDH. We first examined the interaction of free hemin with rGAPDH by UV−visible spectroscopy. At a 1:1 heme:GAPDH tetramer ratio, rGAPDH bound hemin to form a low-spin, six-coordinate complex that is red-shifted with respect to free hemin (Soret band at 385 nm) and possesses a substantially higher molar absorptivity (80 mM^{-1} cm^{-1} vs 58.4 mM^{-1} cm^{-1} for free hemin[33]), as determined using the pyridine hemochrome assay[28,29] (Figure 1A). The ferric rGAPDH−heme complex presents a Soret band with a peak wavelength maximum at 415 nm, indicative of axial coordination to the heme. Reduction of the rGAPDH−heme complex with sodium dithionite generated a species with a Soret band at 425 nm and a sharp α band at 559 nm (Figure 1B), while reaction of the rGAPDH−heme complex with pyridine and dithionite led to the formation of the characteristic band at 556 nm (data not shown).

Analysis of a Cys-null mutant of rGAPDH (all four Cys residues replaced with Ser residues) showed no differences in the spectra compared to that of wild-type rGAPDH, indicating that Cys residues are not directly coordinated to the heme (data not shown). Heme binding affinity (K_d for Cys-null rGAPDH of 21 nM) and gel filtration experiments confirmed that the Cys-null mutant does not differ from wild-type GAPDH in its ability to bind heme (see below). His-Fe-Met-coordinated proteins display an additional band to the red of the Q bands[34−36] that is absent in the spectra of the rGAPDH−heme complex. Finally, the UV−visible spectra of His-Fe-Tyr proteins usually present a Soret band around 406−411 nm in the ferric form,[37,38] which is significantly blue-shifted with respect to the Soret band of the ferric rGAPDH−heme complex (416−420 nm, depending on the pH). These data suggest the ferric GAPDH complex may be bis-His-ligated. We are currently performing mutagenesis to replace each His with Ala or Gly in order to identify the residues involved in heme coordination.

Stability of the rGAPDH−Heme Complex. Gel filtration of the preformed rGAPDH−heme complex was conducted to examine the stability of the complex and the oligomeric state of the protein bound to heme. The results showed that the rGAPDH−heme complex is maintained as a tetramer with a molecular mass of ∼130 kDa (Figure S1A of the Supporting Information). UV−visible analysis of the eluted fractions indicates that the properties of the postcolumn rGAPDH−heme complex are identical to those of the complex prior to gel filtration (Figure S1B of the Supporting Information). This suggests that binding of heme to rGAPDH does not alter the oligomeric state of the protein, and that the rGAPDH−heme complex is relatively stable under these experimental conditions. We found that the rGAPDH−heme complex can be stored at 4 °C for up to 1 month while preserving its spectral properties. The heme bound to rGAPDH could also be detected using an in-gel heme staining method following SDS−PAGE of the complex (Figure S2 of the Supporting Information).

Effect of Heme Binding on GAPDH Secondary Structure and Dehydrogenase Activity. Far-UV circular dichroism was employed to determine whether binding of heme to rGAPDH induced major changes in the protein's

dx.doi.org/10.1021/bi300863a | Biochemistry 2012, 51, 8514−8529

secondary structure. The CD spectrum of native rGAPDH agrees well with previously published results (Figure S3 of the Supporting Information).[39] A comparison of the spectra of apo-rGAPDH and rGAPDH-heme (Figure S3 of the Supporting Information) indicated that heme binding does not substantially alter the secondary structure of the protein. Moreover, we found that heme binding does not affect the dehydrogenase activity of rGAPDH or hGAPDH (data not shown), suggesting that heme binding does not perturb the enzyme's active site.

Binding of rGAPDH to Porphyrin Analogues. We utilized Fe(III)-protoporphyrin IX analogues to investigate the specificity of binding of heme in rGAPDH. A comparison of the UV−visible properties of free and rGAPDH-bound heme analogues is provided in Table 1. We found that Fe(III)-mesoheme, Fe(III)-deuteroheme, and Co(III)-protoporphyrin IX each bound GAPDH to form a red-shifted (with respect to free ligand) complex as we observed for the naturally occurring heme. In contrast, negligible binding was indicated with Fe(III)-2,4-diacetylprotoporphyrin IX, Zn-protorpohyrin IX, and the metal-free protoporphyrin IX. The results suggest (a) a coordinating metal center is required for proper binding of heme to rGAPDH, (b) the axial ligands display a preference for Fe(III) and Co(III) metal centers versus Zn, and (c) the presence of bulky peripheral groups (as in 2,4-diacetylporph) impedes the binding of porphyrin to rGAPDH, implying the existence of a sterically selective heme binding site.

Table 1. Binding of Rabbit GAPDH to Several Protoporphyrin IX Analogues at pH 7.4 (Tris, 100 mM, 10% glycerol) at Room Temperature[a]

	wavelength maxima (nm)	comments
	Free Porphyrin	
protoporphyrin IX (porph IX)	347, 471, 539, 591, 642	
Fe(III)-protoporph IX	352, 392, 497, 613	CT
Fe(III)-mesoporph IX	351, 389, 490, 604	CT
Fe(III)-deuteroporph IX	342, 386, 490, 602	CT
Fe(III)-2,4-diacetyldeuteroporph IX	342, 403, 426 (s), 625	CT
Co(III)-protoporph IX	351, 417, 531, 565	LS
Zn(II)-protoporph IX	347 (s), 393, 550, 589	LS
	GAPDH−Porphyrin Complex	
protoporph IX	347, 471, 539, 591, 642	no binding
Fe(III)-protoporph IX	366, 412, 536	LS, red shift
Fe(III)-mesoporph IX	353, 403, 533	LS, red shift
Fe(III)-deuteroporph IX	344, 404, 531	LS, red shift
Fe(III)-2,4-diacetyldeuteroporph IX	347, 404, 428, 443 (s)	LS, partial binding, red shift
Co(III)-protoporph IX	352, 426, 536, 568	LS, red shift
Zn(II)-protoporph IX	343 (s), 393, 420, 549, 588	LS, partial binding, red shift

[a]CT: charge transfer; LS, low-spin.

Redox Potentiometry. We examined the redox behavior of the preformed GAPDH−heme complex. Stepwise oxidation of the ferrous GAPDH−heme complex with potassium ferricyanide led to the ferric complex. The accompanying spectral change could be fit to the Nernst equation (Figure 2), to yield a calculated midpoint potential (E_m) of −197 ± 9 mV (one-electron transfer; n = 1). Titration of the ferric complex with sodium dithionite displayed marked hysteresis, resulting in deviations of approximately 40−60 mV from the midpoint value determined via the oxidative titration (Figure 2, inset). The reasons for this behavior are currently unknown.

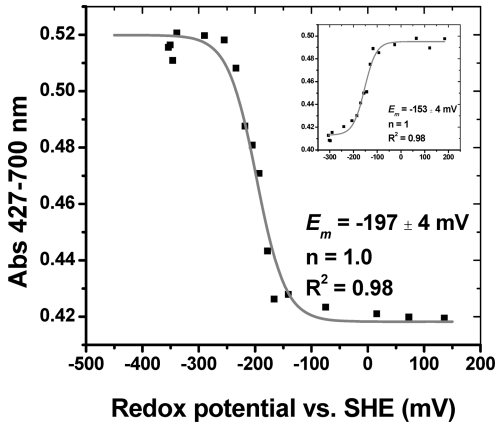

Figure 2. Redox potentiometry of the rGAPDH−heme complex. Oxidative titration of the ferrous GAPDH−heme complex followed at 427 nm (disappearance of ferrous to form the ferric GAPDH−heme complex). The GAPDH−heme complex exhibits Nernst behavior, which could be best fit to a one-electron transfer model with a midpoint potential of −197 ± 4 mV vs SHE. The inset shows the reductive titration of the ferric GAPDH−heme complex. The midpoint potential was −153 ± 4 mV.

Stoichiometry and Binding Affinity of rGAPDH for Heme. UV−visible spectroscopy showed that binding of rGAPDH to heme can involve more than one binding mode. A complex with the aforementioned characteristics forms at high rGAPDH:heme ratios. However, increasing the heme:GAPDH tetramer ratio beyond 1:1 produced a distinct complex with features undistinguishable from those of free hemin in aqueous solution (Figure S4 of the Supporting Information). Nonetheless, the heme moiety was retained under these conditions, as evidenced by desalting experiments. Briefly, G-25 gel filtration of the GAPDH−heme complex obtained upon completion of the titration shown in Figure S4 of the Supporting Information resulted in negligible loss of heme from GAPDH. This suggests that the free hemin-like species detected by UV−visible spectroscopy is associated with the protein. Because under physiological conditions the concentration of GAPDH exceeds that of free heme by several orders of magnitude (~0.03−0.1 μM free heme[40]), we focused on characterizing the binding parameters of the complex that forms when the rGAPDH concentration exceeds the heme concentration. Direct titration of rGAPDH with increasing concentrations of hemin led to the formation of the ferric−rGAPDH complex, with a wavelength peak at 416 nm (Figure 3A). When the rGAPDH tetramer:hemin ratio is <1, a second complex formed with a wavelength maximum at ~400 nm. A fit of the data to the equation given in Materials and Methods yielded the line shown in Figure 3B and gave a calculated dissociation constant (K_d) of 24 nM. A deflection occurs in the line at a stoichiometric value of 1:1 (one heme per GAPDH monomer). Beyond this point, nonspecific binding takes place to form a complex with spectroscopic features that do not differ markedly from those of free hemin. We attempted to crystallize the rGAPDH−heme complex without success. This is possibly due to the existence of multiple heme binding modes.

Heme Binding Kinetics (k_{on} and k_{off}). Binding of heme to rGAPDH was studied by stopped-flow spectroscopy. The

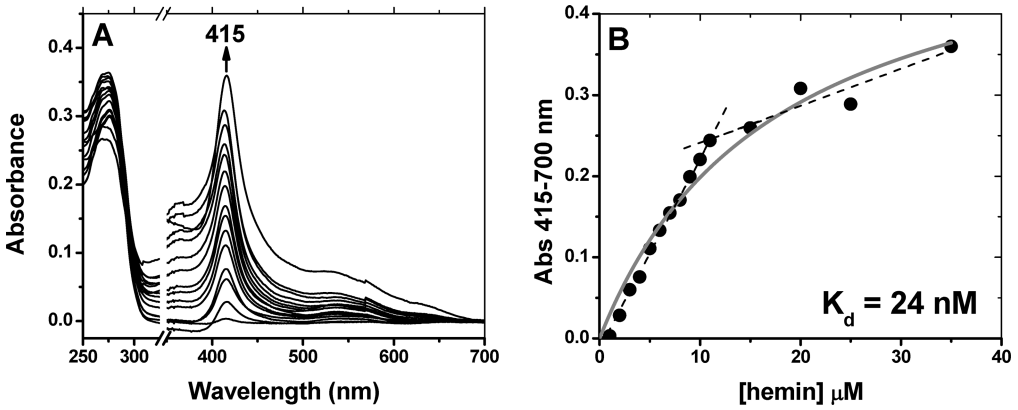

Figure 3. Binding affinity of rGAPDH for hemin. Spectrophotometric titrations were performed by stepwise addition of hemin (0–35 μM) to a 10 μM solution of rGAPDH in buffer (100 mM Tris, pH 7.4, 10% glycerol). A reference was made by stepwise addition of hemin (0–35 μM) to the same buffer. (A) The titration profile (shown as differential spectra, GAPDH–heme complex minus free hemin) displays a maximal change at 415 nm. The break (from 325 to 350 nm) is positioned at 20% of the axis length. (B) Plot of ΔA at 415 nm vs hemin concentration. A deflection point is observed at ~10 μM hemin, indicating that beyond 1:1 rGAPDH:hemin ratios a second, less specific binding occurs.

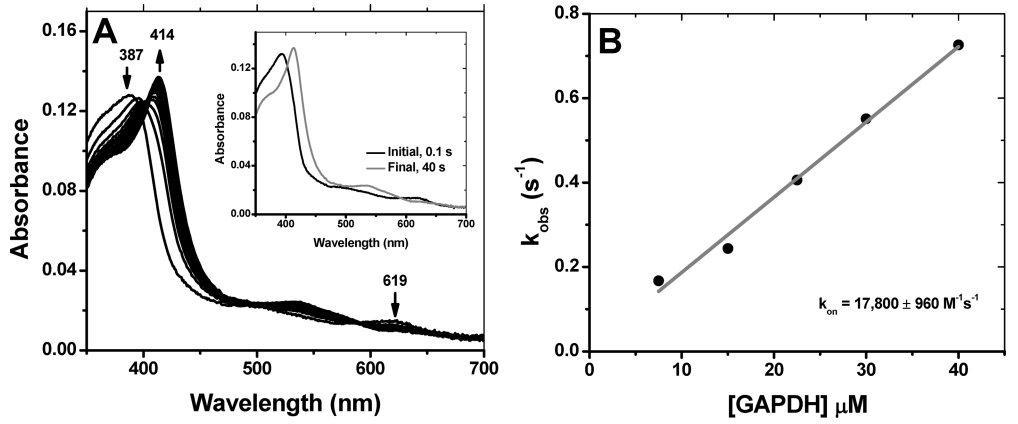

Figure 4. (A) Kinetics of binding of heme to GAPDH. Binding of heme to GAPDH was assessed by stopped-flow spectroscopy. The reaction proceeded cleanly to form the ferric GAPDH–heme complex in a single-step process. The initial and final spectra given in the inset were recorded at 0.1 and 40 s, respectively. (B) Plot of the observed rate constants for different doses of GAPDH yielded a binding constant, k_{on}, of 17800 M^{-1} s^{-1} at 10 °C.

reaction proceeds as a single-step process (Figure 4A) involving two species with isosbestic points occurring at 400 and 590 nm. The spectral data could be fit to a single-exponential equation, and the corresponding k_{obs} values were plotted versus hemin concentration to give a second-order rate constant, k_{on}, of 17800 M^{-1} s^{-1} at 10 °C (Figure 4B). This value is within the range reported for other noncanonical heme binding proteins (Table 2).

The reversibility of binding of heme to rGAPDH was examined using sperm whale apomyoglobin as described in the literature.[41] Binding of heme to rGAPDH was a reversible process. The transfer of ferric heme displayed a biphasic behavior (Figure 5A) with k_{off} rates of 7.0×10^{-3} and 3.3×10^{-4} s^{-1} (at 10 °C). These values lie within the range reported for other noncanonical heme binding proteins (Table 2). Transfer of reduced heme from rGAPDH to apomyoglobin (Figure S5 of the Supporting Information) occurred with a k_{off} of 4.2×10^{-3} s^{-1} at 25 °C, whereas the transfer of ferric heme at the same temperature yielded k_{off} values of 1.4×10^{-2} and 6.9×10^{-4} s^{-1} (Figure 5B). rGAPDH bound very poorly to prereduced heme (Figure S6 of the Supporting Information), with only 18% of the total available reduced heme forming a complex with rGAPDH after 10 min. This suggests that the protein has greater affinity for ferric than ferrous heme.

Reaction of the Ferric and Ferrous rGAPDH–Heme Complexes with Small Ligands. The ferric rGAPDH–heme complex was probed with the classical small ligand molecules utilized to characterize axial substitution in hemoproteins.[42,43] No spectral shift was observed with 100 mM cyanide, 100 mM thiocyanate, or 250 mM imidazole, indicating that these ligands did not bind. The ferrous rGAPDH–heme complex reacted relatively slowly with CO to form a complex with wavelength maxima appearing at 420, 564, and 574 (Figure 6A,B). The reaction profile displayed biphasic behavior. Global analysis of the data using a two-exponential sequential model yielded a k_{obs1} of 1.5 s^{-1} and a k_{obs2} of 0.068 s^{-1} for CO-saturated buffer (final concentration of 1 mM) (Figure 6C). The successive pseudo-first-order constants differed by more than 1 order of magnitude. The fast phase was CO concentration-dependent in a nonlinear manner and showed saturation behavior (Figure 6D). This is the trend expected if association of CO becomes limited by the dissociation of a preexisting endogenous axial ligand. A general mechanism for this reaction is provided in Scheme 1. Thus, binding of CO to ferrous GAPDH can be expressed as

dx.doi.org/10.1021/bi300863a | *Biochemistry* 2012, 51, 8514–8529

Table 2. Kinetic Parameters of Heme Binding Proteins with Various Functions

protein	k_{on} (M^{-1} s^{-1})	k_{off} (s^{-1})	K_d (k_{off}/k_{on}) (M)	K_d (direct) (M)	function	ref
wild-type rGAPDH	1.78×10^4	3.3×10^{-4}	19×10^{-9}	24×10^{-9}	unknown	this work
		7.0×10^{-3}	39×10^{-8}			
nuclear hormone receptor, Rev-erb β (oxidized)	ND[a]	ND[a]	ND[a]	1.17×10^{-7}	gene repression; circadian cycle, inflammation	17
nuclear hormone receptor, Rev-erb β (reduced)	ND[a]	ND[a]	ND[a]	23×10^{-9}	gene repression; circadian cycle, inflammation	17
sperm whale Mb	7.6×10^7	8.4×10^{-7}	1.1×10^{-14}	ND[a]	O_2 transport	65
HRI (heme-regulated inhibitor), eIF2α	1.1×10^7	1.5×10^{-3}	1.4×10^{-10}	ND[a]	regulation of protein synthesis by iron	69
BSA	5.0×10^7	1.1×10^{-2}	2.2×10^{-10}	ND[a]	fatty acid transport; heme metabolism	65
apo-DHR51-LBD (*Drosophila melanogaster*, homologous to human nuclear receptor Rev-erb α and β)	ND[a]	ND[a]	ND[a]	4.3×10^{-7}	nuclear receptor	91
CcmE	ND[a]	ND[a]	ND[a]	2×10^{-7} (high affinity), 10×10^{-6} (low affinity)	heme chaperone; cytochrome *c* biogenesis in Gram-negative bacteria	92
HasAp	1.6×10^7	ND[a]	35×10^{-6}	ND[a]	heme acquisition from Hb in *Pseudomonas aeruginosa*	37
HtsA	8×10^7	ND[a]	8×10^{-6}	ND[a]	heme acquisition by *Streptococcus pyogenes*	93
Shp	1.6×10^6	ND[a]	22×10^{-6}	ND[a]	cell surface hemin transfer protein in *S. pyogenes*	94
HemQ	ND[a]	ND[a]	ND[a]	$30-40 \times 10^{-6}$	Heme synthesis by *Mycobacterium tuberculosis*	80
HTP (PhuT)	ND[a]	3.8×10^{-4}	ND[a]	0.0012	heme acquisition by *P. aeruginosa*	24
PhuS	1.8×10^5	3.6×10^{-2}	0.2×10^{-6}	ND[a]	heme acquisition by *P. aeruginosa*	66
pa-HO	1.1×10^5	6.6×10^{-2}	0.6×10^{-6}	ND[a]	heme degradation by *P. aeruginosa*	66
Rv0203	1.3×10^8	8.2×10^{-2}	6.2×10^{-10}	ND[a]	heme binding protein *M. tuberculosis*	95

[a]Not determined.

$$k_{obs} = \frac{k_{-Y}k_{CO}[CO]}{k_Y + k'_{CO}[CO]} = \frac{k_{-Y}[CO]}{k_Y/k'_{CO} + [CO]} \quad (2)$$

where Y is the distal axial ligand that undergoes displacement by CO. The fitting of eq 2 to the data for the fast phase (k_{obs1}) gives an axial ligand dissociation rate constant k_{-Y} of ~2 s^{-1} and a ligand rebinding rate ratio (curvature), k_Y/k'_{CO}, of ~0.1 mM. A similar rebinding rate ratio was reported for the displacement of Cys^{52} by CO in CBS (106 μM).[44]

The slow phase of CO binding had a much smaller amplitude than the fast phase and did not display a clear CO concentration dependence. We attribute this second phase to a minor subpopulation of the ferrous GAPDH−heme complex with more stable axial ligand association. An additional, spectroscopically different rGAPDH−heme−CO complex forms when the reaction is conducted at an rGAPDH tetramer:heme ratio of <1:1. This complex presents a Soret band at 410 nm, and its rate of formation was 4-fold faster than that of the rGAPDH−heme−CO complex at 420 nm (Figure S7 of the Supporting Information).

The ferrous rGAPDH−heme complex also reacted with NO to form a stable, long-lived pentacoordinate complex with a Soret band appearing at 385 nm (Figure 7A and its inset). As observed for CO, binding of NO could be best fit to a two-exponential model, with a k_{obs1} of 0.66 s^{-1} and a k_{obs2} of 0.014 s^{-1} under conditions of NO saturation (Figure 7B). The reaction of the preformed Fe(II)−NO−rGAPDH complex with dioxygen was slow and led to the formation of the ferric GAPDH−heme complex as the final product (Figure 8A and its inset). Under conditions of O_2 saturation, the observed rate constant for the reaction of the Fe(II)−NO−rGAPDH complex with dioxygen to form the ferric GAPDH−heme complex was 0.001 s^{-1} (Figure 8B).

Magnetic Circular Dichroism. UV−visible absorption and MCD spectroscopies were employed to help establish the coordination structure of heme bound to GAPDH as well as the changes in ligation due to heme oxidation and/or reduction and the addition of small exogenous ligand molecules.

The spectral comparison of ferric rGAPDH to two bis-His examples, cytochrome b_5 and H93G(bis-Im) sperm whale Mb, is shown in Figure 9A.[1,2] The spectra of ferric rGAPDH are in good agreement with those of both bis-His examples even though the MCD features in the Soret region are slightly red-shifted (4−6 nm) and are the least intense of the three systems. The MCD bands in the visible region of all three derivatives are also similar. The major UV−vis absorption peaks of ferric rGAPDH are slightly red-shifted when compared to those of cytochrome b_5 and H93G(bis-Im) Mb, and the Soret peak intensity is the lowest of the three. Nonetheless, the UV−vis absorption and MCD spectra of ferric rGADPH are generally similar to those of the two ferric bis-His-ligated complexes. This suggests that ferric rGAPDH has a similar bis-His coordination structure.

To study ferrous rGAPDH, the protein was reduced using a minimal amount of sodium dithionite. This reduction was judged to be complete when the UV−vis absorption spectra

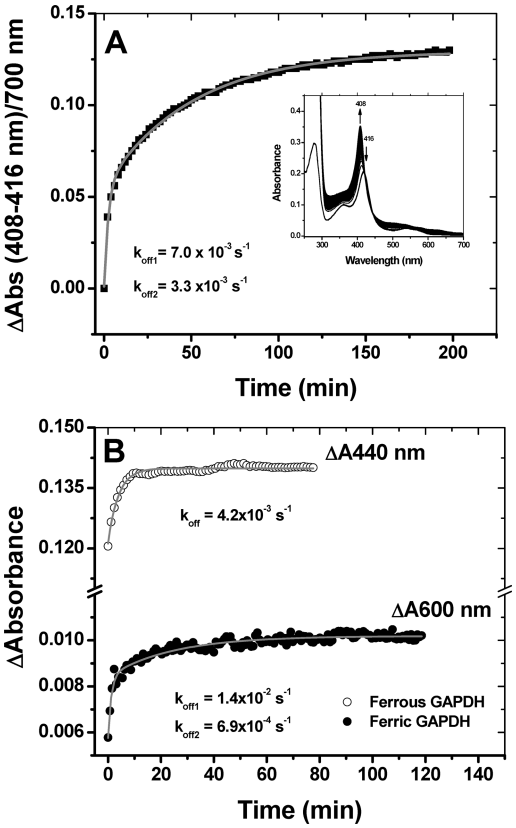

Figure 5. Transfer of heme from GAPDH to apomyoglobin. Binding of heme to GAPDH is a reversible process. (A) Incubation of the ferric GAPDH−heme complex with a 5-fold excess of apomyoglobin resulted in the stoichiometric transfer of heme with rates of 7.0×10^{-3} and 3.3×10^{-4} s^{-1} at 10 °C (biexponential fit). (B) Time courses for transfer of ferric and ferrous heme to apomyoglobin at 25 °C. The transfer of heme from ferrous GAPDH to apomyoglobin was derived from the absorption changes at 440 nm (maximal absorption for ferrous Mb) and was best fit to a single-exponential equation. In panel B, the transfer of heme from ferric GAPDH to apomyoglobin was derived from the absorption changes at 600 nm (charge transfer band of holo-Mb) to give k_{off} rates of 1.4×10^{-2} and 6.9×10^{-4} s^{-1}.

had shifted from 420 nm for the Fe(III) heme to 427 nm for the Fe(II) system. The ferrous rGAPDH was once again compared to cytochrome b_5. The overlaid spectra are shown in Figure 9B. The UV−vis and MCD spectra of ferrous rGAPDH resemble those of the ferrous cytochrome b_5 bis-His system.[1] In the visible region, the peak-to-trough MCD intensity of the spectrum of ferrous rGAPDH compares especially well with that of cytochrome b_5. The UV−vis absorption spectrum of ferrous rGAPDH is also similar to that of the bis-His-ligated complexes. The Soret absorption peak of ferrous rGAPDH is once again slightly red-shifted compared to that of ferrous cytochrome b_5. The UV−vis absorption spectra of the ferrous proteins in the visible region feature sharp, defined α and β bands for each protein. The position of the β band for rGAPDH at 531 nm is identical to that of cytochrome b_5. The more pronounced α bands of the two systems are very similar in intensity as well as in relative position, with the α band of ferrous rGAPDH (559 nm) located slightly to the red of that of ferrous cytochrome b_5 (555 nm). The close spectral similarities between ferrous cytochrome b_5 and rGAPDH again favor bis-His ligation in the latter.

The ferrous−CO−rGADPH complex was also studied with UV−vis and MCD spectroscopy. The spectra of the Fe(II)−CO−rGADPH complex and sperm whale Mb are shown in Figure 9C. The spectra of the ferrous−CO−rGAPDH complex have characteristics very similar to those of the His−Fe−CO complex present in H93G Mb.[3] Upon analysis of the UV−vis data, the spectra of the ferrous−CO−rGAPDH complex are blue-shifted compared with those of the ferrous−CO complexes of native Mb and the Mb H93G mutant (data not shown); however, the visible region shows that the rGAPDH has fully converted to a Fe(II)−CO species because of the change in relative intensities for the α and β bands. The most noticeable spectral difference for the Fe(II)−CO complex is seen with the rGAPDH α band, which is blue-shifted by 12 nm when compared to that of native Fe(II)−CO Mb. Nevertheless, the relative intensity and shape of the α bands are comparable throughout, consistent with His−Fe−CO ligation.

Resonance Raman Analysis of Ferric, Ferrous, and Ferrous−CO−rGAPDH−Heme Complexes. We utilized resonance Raman to further examine the electronic environment of the heme bound to rGAPDH. Figure 10 shows the rR spectra of ferric, ferrous and ferrous−CO−rGAPDH−heme complexes in the low- and high-frequency regions (panels A and B, respectively).

The ferric GAPDH complex is clearly a low-spin, six-coordinate (LS-6c) species. This is particularly indicated by the frequency of the ν_3 band at 1504 cm^{-1}. The frequencies of the ν_2−ν_4 and ν_{10} modes are compatible with bis-His coordinated heme. The bands at 1630 and 1640 cm^{-1} are reminiscent of bis-His globins[45−47] and other bis-His complexes,[48,49] respectively; however, this assignment is somewhat speculative because of the superimposition of several modes (ν_{10} and vinyl stretching modes) of possibly different species.

The oxidation state, π^* electron density band ν_4, occurs at 1373 cm^{-1} in the ferric rGAPDH−heme complex and at 1359 cm^{-1} in the reduced rGAPDH−heme complex, confirming the ferric state of the native GAPDH−heme complex and its complete reduction to the ferrous form upon addition of dithionite. The value of the ν_4 frequency is a good indication that the proximal ligand is a histidine residue. Additionally, the presence of different ν_3 bands at 1470 cm^{-1} [high-spin, five-coordinate (HS-5c)] and 1492 cm^{-1} (LS-6c) indicates the presence of multiple species, which might arise from photolysis, thermal equilibrium, or heterogeneity of heme−protein complexes. The nature of this equilibrium is currently under investigation. A summary of all the rR stretching values is provided in Table 3. These spectral features are consistent with previously characterized bis-His coordinated hemes.[50,51]

We recorded the resonance Raman spectrum of the Fe^{II}−CO complexes for wild-type rGAPDH and a series of mutants. All spectra of the Fe−CO complex seem also to correspond to a mixture of various Fe^{II} and Fe^{II}−CO species (ν_4 at 1359/1372 cm^{-1}), indicating photodissociation of CO upon irradiation. Further evidence of weak distal axial ligation was provided by the concomitant presence of HS-5c Fe^{II} and LS-6c Fe^{II}−CO complexes (ν_3 at 1465/1496 cm^{-1}) under these conditions. The observed frequencies match the ones reported for 6c-LS (Fe^{II}−CO) bis-His of neuroglobin (1374/1497 cm^{-1}).[45] The analysis of the frequencies of the Fe−CO and C−O stretching modes provides insight into the proximal ligation. Indeed, carbon monoxide is a σ-donor and a π-acceptor ligand when bound to heme. The back-donation from the iron d π^* orbital to the empty antibonding π^* CO orbital results in a

dx.doi.org/10.1021/bi300863a | Biochemistry 2012, 51, 8514−8529

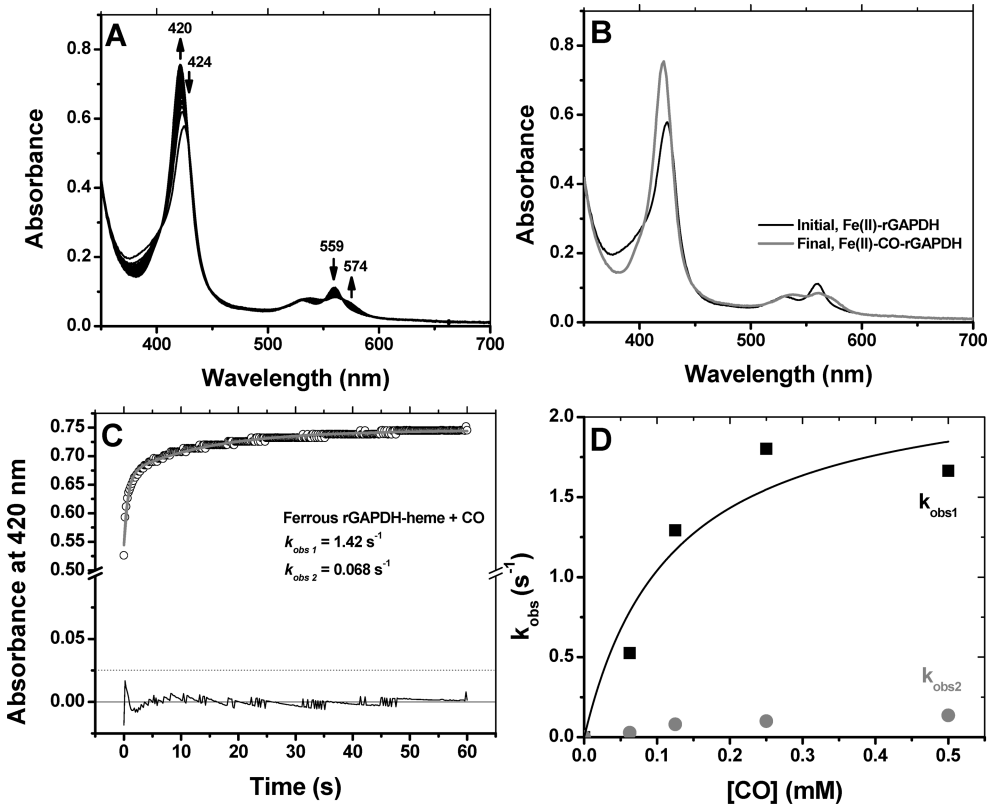

Figure 6. Reaction of ferrous GAPDH with CO. The reaction of ferrous GAPDH with CO was examined by stopped-flow kinetics at 10 °C. (A and B) Reaction profile and initial and final species detected by global analysis, respectively. (C) Time course at 420 nm for the formation of the ferrous−CO complex under conditions of CO saturation (final concentration of 0.5 mM). (D) Dependence of k_{obs} (average of two independent experiments) on the dose of CO. The observed rate varied with the dose of CO in a nonlinear manner and displayed saturation behavior.

Scheme 1. General Mechanism for Distal Ligand Displacement by CO in the GAPDH−Heme Complex

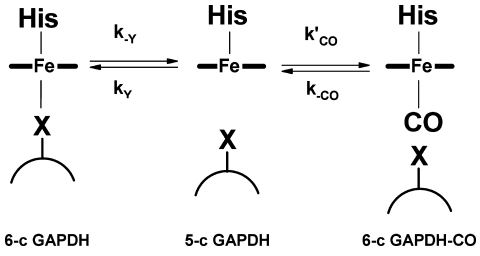

strengthening of the Fe−CO bond and a weakening of the C−O bond.[52−55] Thus, changes in the electrostatic and polar properties of the heme distal pocket will modify this back-donation and lead to an inverse linear correlation between the ν(Fe−CO) and ν(C−O) frequencies. However, changes in the electron donating properties of the proximal ligand induce a σ-competition between the σ donor orbitals of CO and of the proximal ligand for the iron orbital, leading to a modification of the ν(Fe−CO) frequency and a shift of the correlation curve. As a result, heme−CO complexes of proteins with similar proximal ligands align on the same ν(Fe−CO)/ν(C−O) correlation curve.[52−54] The frequency of the ν(Fe−CO) mode is observed at 493 cm^{-1} for the wild type and all mutants, while the ν(C−O) stretch appears at 1965−1967 cm^{-1} for most of the samples and is poorly enhanced for the others [including the wild type (data not shown)], which is reminiscent of Fe−CO complexes described for other His-ligated proteins.[50,51] Plotting these values on the ν(C−O)/ν(Fe−CO) correlation graph[54] shows that the GAPDH−heme complex falls right on the correlation line for His-ligated heme.[52−54]

However, bis-His ligated proteins often display (at least) two different Fe−CO conformations[46] characterized by two different ν(Fe−C) frequencies around 493 and 523 cm^{-1}. Removal of the distal His by mutagenesis was shown to lead to the disappearance of the 523 cm^{-1} band, which suggested that this conformer is characterized by an H-bond (or electrostatic) interaction between the CO ligand and the distal histidine that remains in the heme pocket.[46] In our case, the presence of a single band at 493 cm^{-1} (as observed in the GAPDH−heme complex) supports a His-free distal environment that could be attributed either to the displacement of the distal His (far) from the heme or to a weak distal ligand other than histidine.

Electronic Paramagnetic Resonance of the Ferric rGAPDH−Heme Complex. To further examine the electronic environment of the heme bound to rGAPDH, we collected X-band EPR measurements on the ferric heme complexes of rGAPDH and the Cys-null mutant. In the high-field region, the spectrum of the wild-type complex presents resonances at g values of 2.95, 2.49, 2.26, and 1.89, consistent with two low-spin, six-coordinate binding modes with principal values of 2.95, 2.26, and 1.89 and tentative values of 2.49, 2.26, and 1.89 (Figure 11). The signature g value of the first species with a g_{max} at 2.95 is consistent with bis-His ligation, whereas the resonance at 2.49 could be tentatively assigned to a His−Fe−Cys binding mode. However, the EPR spectrum of the Cys-null mutant did not differ markedly from that of wild-type rGAPDH (Figure 11), indicating that Cys is not involved in the ligation

dx.doi.org/10.1021/bi300863a | *Biochemistry* 2012, 51, 8514−8529

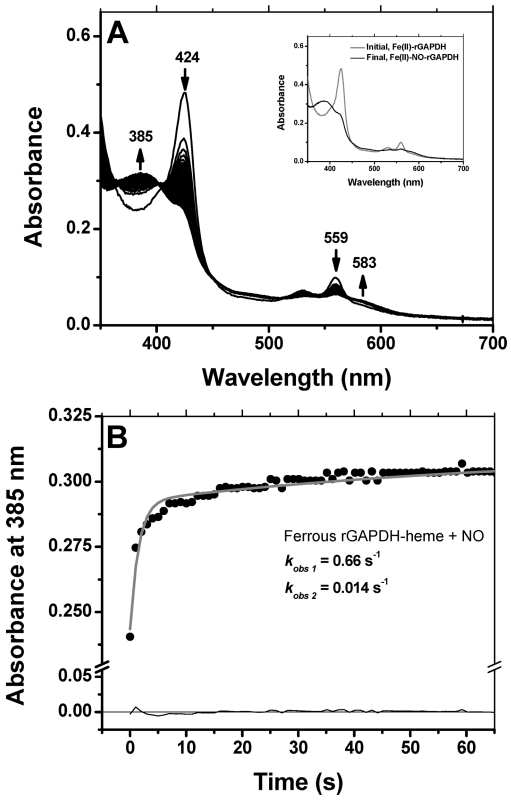

Figure 7. Reaction of ferrous GAPDH with NO. The reaction of ferrous GAPDH with NO was monitored by stopped-flow kinetics at 10 °C. (A) Reaction of ferrous GAPDH with NO led to the formation of a stable, 5-coordinate complex featuring a broad Soret band at 385 nm. The inset shows the spectra of the initial and final species. (B) As observed for CO binding, the reaction with NO displayed biphasic behavior; thus, the reaction time course could be best fit to a sequential two-exponential model.

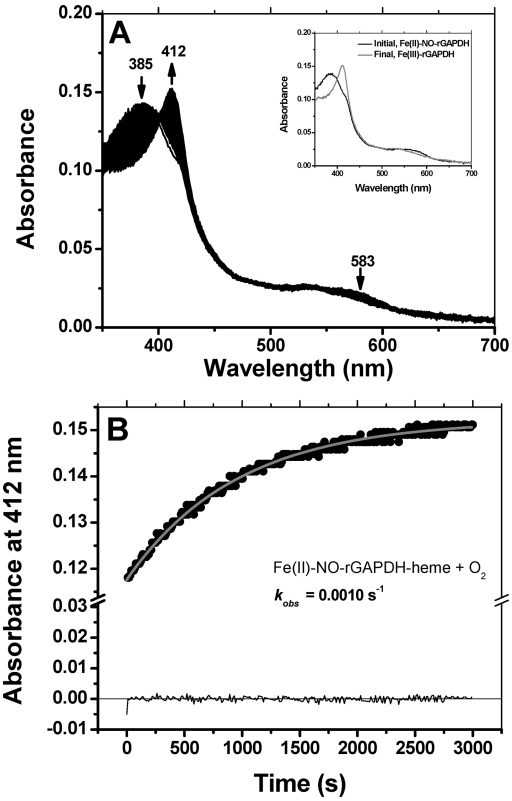

Figure 8. Reaction of the ferrous GAPDH−NO complex with dioxygen. The ferrous GAPDH−NO complex reacted slowly with dioxygen to form the ferric GAPDH−heme complex. An estimated k_{obs} of 0.0010 s^{-1} was determined at 10 °C, in oxygen-saturated buffer.

of heme in either complex. In addition, signals in the low-field region with g = 4.30 (nonspecific iron) and g = 6.03 (high-spin ferric heme, likely from uncoordinated hemin) features are also observed by EPR.

Chemical Characterization. Treatment of rGAPDH with DEPC (an agent that modifies His residues by ethoxylation) hampered heme binding completely, whereas the addition of DEPC to the preformed rGAPDH−heme complex had no effect on its spectral properties (Figure 12). These results suggest that heme coordination by rGAPDH is accomplished via one or two His residues, and that once the complex forms, at least one axial His can no longer be modified by DEPC.

Isolation of Heme-Bound rGAPDH and Heme Binding to GAPDHs from Other Species. Because rGAPDH is not a canonical heme binding protein (it does not possess a defined heme binding site), we set out to examine (a) whether the rGAPDH−heme complex could be isolated in vivo and (b) whether heme binding is common among GAPDH proteins from different species. *E. coli* overexpressing rabbit, human, or *S. suis* GAPDHs was grown in the presence or absence of the heme precursor δ-aminolevulinic acid (δ-ALA). The proteins were purified and examined for heme content by UV−visible spectroscopy. Figure S8 (Supporting Information) shows the UV−visible spectra of human (panel A) or *S. suis* (panel B) GAPDH from cultures grown in the absence or presence of δ-ALA. We found that under conditions where heme synthesis is stimulated a measurable fraction of the intracellular GAPDH appears to be heme-bound (2−8%).

DISCUSSION

Reports that GAPDH participates in hemoprotein maturation[14] and binds to hemin−agarose affinity resins[10,11] prompted us to investigate the GAPDH−heme interaction in detail. We found that forms of GAPDH from three different species [*Homo sapiens*, *Oryctolagus cuniculus*, and *S. suis* (amino acid sequence alignment in Figure S9 of the Supporting Information)] all contained some bound heme when they were expressed and purified from bacterial cells and could also bind substoichiometric amounts of heme provided to their purified apo forms, to generate a low-spin, six-coordinate complex with spectral features very similar to those of hemoproteins featuring bis-His axial coordination.[36,56,57] For example, the UV−vis and MCD spectra of the rGAPDH−heme complex matched the spectra of two well-known bis-His coordinated systems (cytochrome b_5 and sperm whale Mb[1−3]) with regard to the position and intensity of the Soret and α/β bands for the ferric, ferrous, and ferrous−CO states.

Similarly, the resonance Raman fingerprints of the Fe^{III}, Fe^{II}, and $Fe^{II}CO$ species of the rGAPDH−heme complex, along with the ν(Fe−CO)/ν(C−O) correlation, strongly support a His ligation of the heme with some characteristics reminiscent of the bis-His complex. The spectral properties of a Cys-null GAPDH mutant ruled out alternative Cys axial coordination to the heme, and chemically modifying the His residues of GAPDH prevented heme from binding. The selectivity that GAPDH displayed toward the porphyrin metal center (good

dx.doi.org/10.1021/bi300863a | *Biochemistry* 2012, 51, 8514−8529

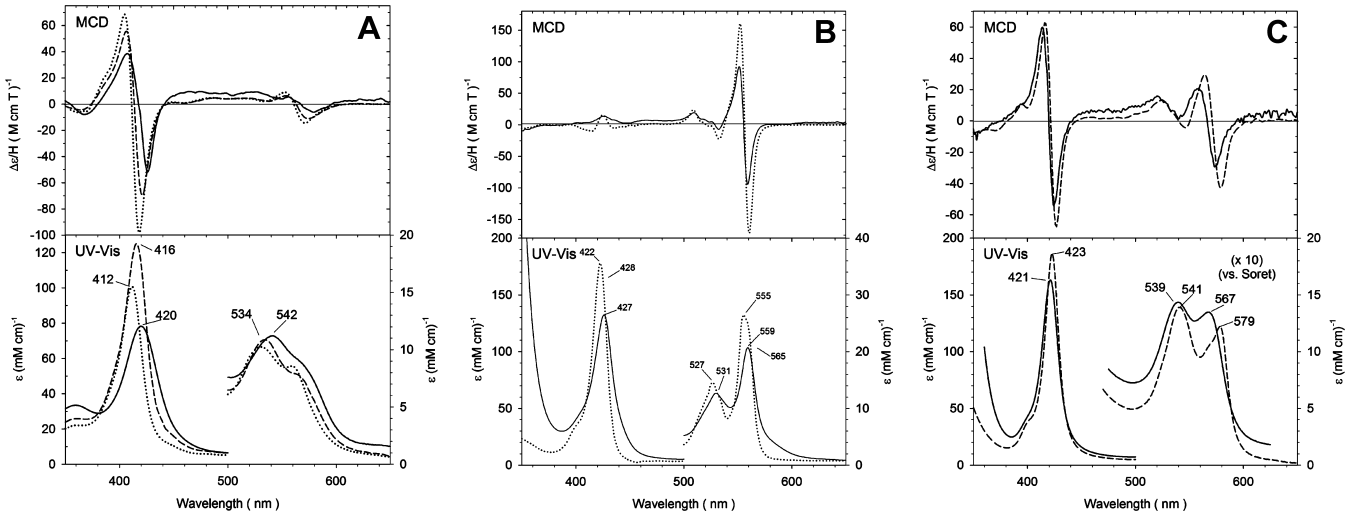

Figure 9. MCD and UV−vis spectra of the GAPDH−heme complex and model systems cytochrome b_5 and sperm whale Mb. (A) Spectra of the ferric GAPDH−heme complex (—) at pH 7.8, cytochrome b_5 (···), and (bis-Im) H93G Mb (---). Spectra of ferric cytochrome b_5 are replotted from ref 1, and spectra of ferric (bis-Im) H93G Mb are replotted from ref 2. (B) Spectra of the ferrous GAPDH−heme complex (—) and cytochrome b_5 (···). Spectra of ferric cytochrome b_5 are replotted from ref 1. (C) Spectra of ferrous−CO complexes of GAPDH (—) and H93G-Im Mb (---). Spectra of the ferrous−CO complex of H93G-Im Mb are replotted from ref 3.

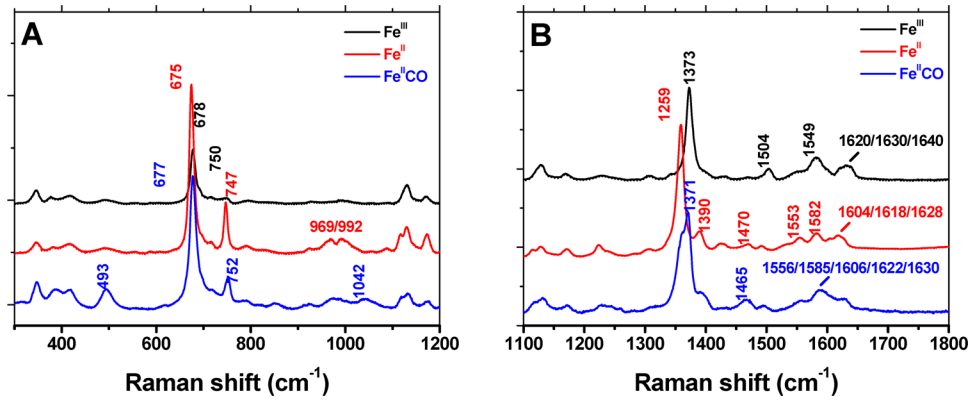

Figure 10. Resonance Raman spectra of ferric, ferrous, and ferrous−GAPDH−CO complexes. The high-frequency region of the spectrum of the GAPDH−heme complex was obtained with laser excitation at 406 nm. The observed bands are consistent with a low-spin, six-coordinate complex, with at least one His as the axial ligand.

Table 3. Resonance Raman Shifts for the Ferric, Ferrous, and Ferrous−CO Complexes of the rGAPDH−Heme Complex

Low-Frequency Region of the Spectrum of the rGAPDH−Heme Complex													
Fe^{III}	WT	346	382	419	494	546/559/587	678	692/715	750	1055	1121	1132	1171
Fe^{II}	WT	346	381	417	493	–	675	697/717	747	–	1117	1130	1174
$Fe^{II}CO$	WT	347	385	418	493	–	677	698/719	752	1042	1117	1133	1172
High-Frequency Region of the Spectrum of the rGAPDH−Heme Complex													
Fe^{III}	WT	1373	1397	1469	1489	1504	1549	1582	1600	1620	1630	1639	
Fe^{II}	WT	1359	1390	1470	1491	–	1553	1582	1604	1618	1628	–	
$Fe^{II}CO$	WT	1371	1393	1465	1496	–	1556	1585	1606	1622	1630	–	

binding with Fe or Co but not with Zn) was also consistent with bis-His axial ligation. Finally, the midpoint potential of the GAPDH−heme complex (−197 mV) is comparable to those of other bis-His coordinated proteins,[43,58,59] which generally have lower midpoint potentials than hemoproteins containing other axial ligands, such as members of the cytochrome *c* family, cellobiose dehydrogenase, and Mb with H_2O/His as axial ligands.[34,58,60,61]

Interestingly, X-band EPR results suggested the presence of two different heme-bound rGAPDH populations: one that was consistent with bis-His coordination with *g* values of 2.95, 2.26, and 1.89 and a second population of unknown nature with a prominent g_{max} value at 2.49. Some uncoordinated hemin is also observed. A similar X-band EPR pattern was reported for two other proteins, namely, the bacterial iron response regulator (Irr)[62] and the nuclear hormone receptor Rev-erb β.[17] In these cases, the existence of two distinct heme-bound populations was attributed to heterogeneity of the heme binding modes and redox-dependent switching of the axial ligands. According to the data gathered by other spectroscopic techniques used in

dx.doi.org/10.1021/bi300863a | *Biochemistry* 2012, 51, 8514−8529

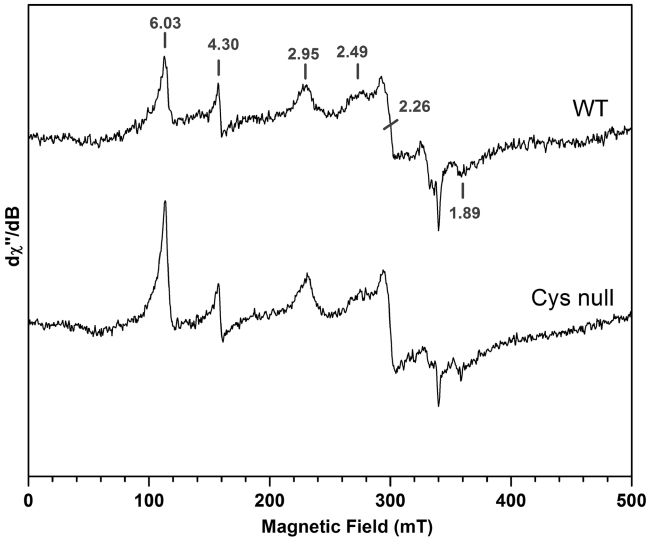

Figure 11. X-Band EPR spectra of ferric heme–wild type and –Cys–null rGAPDH complexes. The data suggest that two heme subpopulations are present under these conditions, one of which is consistent with bis-His axial ligation (g = 2.95, 2.26, and 1.89). The nature of the species displaying a g value of 2.49 is currently unknown. The spectra were recorded at 10 K using a 2 mT field modulation amplitude, a 0.5 mW microwave power, and a 9.4956 GHz microwave frequency.

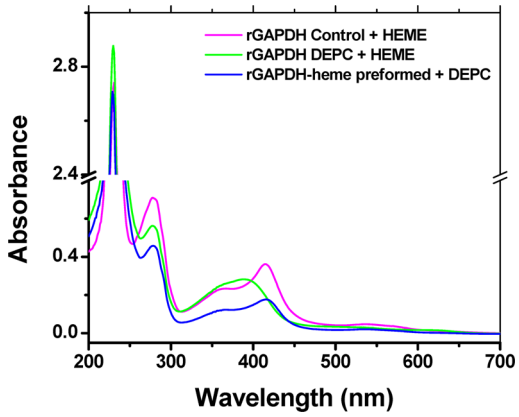

Figure 12. Modification of His residues with DEPC. Untreated (control), heme-free, and preformed GAPDH–heme complexes were treated with 15 mM DEPC for 2 h on ice. The samples were buffer-exchanged to remove excess DEPC and tested for their ability to bind hemin. DEPC-treated GAPDH was unable to bind heme. Treatment of the preformed GAPDH–heme complex with DEPC does not alter the UV–vis spectral properties of the complex.

this study, the two GAPDH–heme populations observed by EPR are probably due to heterogeneity in the conformation or location of the heme binding sites.

The ferric rGAPDH–heme complex was stable over several days at 4 °C and only partly dissociated during gel filtration or while the GAPDH–heme complex was run on nonreducing SDS–PAGE gels.[24,63] Our titration and kinetic studies confirmed that rGAPDH binds heme avidly, with a K_d of 24 nM and a k_{on} of 1.75×10^4 M^{-1} s^{-1}. On the basis of the K_d value and the estimated intracellular levels of free hemin (0.03–0.1 μM[40]) and GAPDH (1–100 μM[64]), a fraction of GAPDH could indeed exist in the heme-bound form, which we confirmed in our bacterial expression studies. Despite the stability of the ferric rGAPDH–heme complex, its heme moiety could be transferred to apomyoglobin with a k_{off1} of 7.0×10^{-3} s^{-1} and a k_{off2} of 3.3×10^{-4} s^{-1} at 10 °C. Dissociation of heme from GAPDH was slower than that reported for BSA-bound heme (10^{-2} s^{-1} [65]) or for the cytoplasmic heme binding protein PhuS (3.6×10^{-2} s^{-1} [66]) but faster than the heme loss rates of most globins (10^{-4} to 10^{-6} s^{-1} [41,67]) and nitrobindin (3.6×10^{-5} s^{-1} [68]) (Table 2). The ability of rGAPDH to bind heme in a reversible manner with intermediate affinity makes it plausible to act as a heme sensor or transient heme carrier in vivo. Indeed, similar k_{off} rates for hemin were reported for eIF2α kinase (1.5×10^{-3} s^{-1}), which exploits heme sensing to control protein synthesis.[69]

Treatment of apo-rGAPDH with DEPC, an agent that specifically blocks His residues (and to a much lesser extent Tyr and Lys residues),[70−73] abolished the protein's ability to bind heme. However, DEPC treatment of a preformed rGAPDH–heme complex did not alter the spectral properties of the complex, suggesting the axial His residue(s) was unable to react. This is consistent with cyanide, azide, or imidazole being unable to bind to the ferric rGAPDH–heme complex and suggests a relatively stable bis-axial coordination to ferric heme. Our CO binding studies suggest that the bis-axial coordination may be weakened in the ferrous state. Still, CO binding was relatively slow and appeared to require displacement of a coordinating ligand. A similar behavior with CO has been reported for HtsA, a His/Met coordinated hemoprotein,[74] cystathionine-b-synthase,[44] and CooA.[75] Overall, our data are consistent with a relatively stable ferric heme bis-coordinated complex that when reduced allows one of the axial ligands to become displaced by CO according to the mechanism depicted in Scheme 1. The ferrous GAPDH–heme species also bound NO to form a complex whose spectral features and slow reaction with O_2 (0.001 s^{-1}) identified it as a five-coordinate ferrous heme–NO complex.[76] NO binding was slow and biphasic like we observed for CO, consistent with NO binding also requiring displacement of an axial ligand. Indeed, the upper rates of CO and NO binding likely approximate the dissociation rate of an axial ligand in the ferrous GAPDH–heme complex. We observed that the reaction of dioxygen with the preformed GAPDH–heme nitrosyl resulted in the enzyme returning to its characteristic ferric heme-bound state, without the formation of any detectable intermediates (His–Fe–NO, His–Fe–O_2, etc.). Thus, oxidation of the GAPDH–heme nitrosyl seems to occur via a mechanism in which religation by the axial residues does not generate detectable intermediates.

Interestingly, preformed ferrous heme bound very poorly to GAPDH. In addition, the transfer of ferrous heme from GAPDH to apomyoglobin was slightly faster than for ferric heme. Hargrove et al. showed that the major factors contributing to the rate of heme loss from a protein are solvent exposure and the number and types of protein–heme contacts.[41,67] If heme reduction weakens the bis-axial ligation, this could help explain the faster k_{off} of the ferrous heme from GAPDH. Because the E_m value for the GAPDH–heme complex is within reach of most cellular reductants,[77] a redox-based change in heme affinity, mediated through the bis-axial coordination, could potentially facilitate the release of heme from GAPDH in the intracellular milieu.

When heme:GAPDH ratios exceeded one heme per tetramer, an additional complex formed with properties resembling those of a pentacoordinate species. A similar phenomenon has been reported for prostaglandin G/H

dx.doi.org/10.1021/bi300863a | Biochemistry 2012, 51, 8514–8529

synthase,[78] histidine rich protein 2,[79] the bacterial iron response regulator (Irr),[62] and the heme synthesis protein HemQ.[80] Although this type of GAPDH−heme complex is unlikely to exist under physiological conditions where the concentration of GAPDH exceeds that of free heme, it was still of interest to examine its properties. The pentacoordinate species formed an Fe(II)−CO complex whose Soret absorption maximum was blue-shifted (410 nm vs 420 nm for the six-coordinate, low-spin rGAPDH−heme complex that forms at heme:GAPDH ratios of ≤1:4) and whose rate of formation was ∼4 times faster ($k_{obs,5\text{-}coord,410\ nm}$ = 4.3 s^{-1} at a saturating CO concentration vs $k_{obs,6\text{-}coord,420\ nm}$ = 1.2 s^{-1} at a saturating CO concentration), all consistent with there being a weaker axial ligand in place of His for the bound heme in this case.

A thorough examination of the heme binding capacity of various proteins not reported to bind heme showed that they associated with the cofactor with similar strengths as described for Per2 and nPas2, two circadian rhythm proteins proposed to utilize heme to attain their regulatory functions.[81] Extensive mutagenesis of the PAS domain thought to be involved in heme binding did not abolish the protein's ability to bind heme. This led Airola et al. to conclude that the interaction between heme and Per2 is likely nonspecific, mainly occurring via hydrophobic interactions and exposed ligands on the surface of the protein.[81] According to Hayasaka et al.,[71] the fact that extensive mutagenesis failed to eliminate the heme binding ability of Per2 and nPas2 is not surprising as the structures of heme responsive heme sensor proteins exhibit an enhanced flexibility, which allows for facile ligand switching in the immediate neighborhood of the heme.[71] Further, for proteins whose function requires relay of the heme onto other targets or quick binding reversibility, the existence of a heme binding site near the surface is a valuable feature rather than a sign of nonspecificity as suggested by Airola et al.[81]

The function of heme-bound rGAPDH is currently unknown. One major factor affecting heme binding is its nonspecific partitioning into hydrophobic regions of the protein,[82] which also dictates the tendency of heme to adsorb to a variety of proteins.[65,83−87] In contrast, specific binding of heme is governed by the formation of bonds with side chains of amino acids positioned near the porphyrin ring.[88,89] However, the presence of a canonical, well-defined heme binding site does not guarantee stable or constitutive binding of heme to a protein. For example, HemQ, an essential protein for the biosynthesis of heme in Gram-positive bacteria, possesses a canonical heme binding site similar to that present in chlorite dismutase,[80] yet the recombinant protein is isolated with only small and variable amounts of heme. Reconstitution of the holoprotein requires the addition of exogenous hemin during the workup procedure.[80] The authors reported poor heme binding and noted that HemQ is either capable of binding more than one heme per subunit or the multimeric protein does not have uniform heme binding affinity.[80] Recently, Hamza et al. made the distinction that a dedicated heme binding protein can be defined as such only if its binding is specific for heme, i.e., if the protein does not bind to metal-free protoporphyrin IX.[90]

On the basis of our results, it is reasonable to propose that the specificity and reversibility of heme binding to GAPDH may serve at least three possible functions. (a) It may exploit binding specificity to perform heme sensing functions. (b) It may prevent free heme from binding to other proteins while in transit to its destination. (c) It may act as a transient trap to diminish the intracellular reactivity and potential toxicity of free heme. Indeed, the relative stability of the ferric GAPDH−heme complex and its poor reactivity toward small ligands may have evolved to limit the reactivity of the free heme pool during intracellular trafficking events. GAPDH may thus operate as a chaperone to control the serendipitous reactivity and toxicity of heme prior to its downstream delivery. On the other hand, the relative instability of the ferrous GAPDH−heme complex and its capacity to bind NO may function as a signal to trigger downstream processes. Along these lines, a previous report by our laboratory indicated that the proposed interaction of GAPDH with heme in cultured cells was weakened by treatment with a NO donor, and this was associated with an inhibition of insertion of heme into apo-NOS.[14] We found evidence that this process was mediated by S-nitrosylation of GAPDH.[14] In lieu of our current findings, we can also consider that NO might influence GAPDH behavior during cellular heme insertion by coordinating to the GAPDH−heme complex. Our study provides a platform for testing this possibility.

■ ASSOCIATED CONTENT

Supporting Information

Pyridine hemochrome UV−visible spectra, in-gel heme staining, heme spectrophotometric titrations, reaction of GAPDH with ferrous heme, reaction of ferrous GAPDH with CO, and UV−visible spectra of heme-bound native human and *S. suis* GAPDH. This material is available free of charge via the Internet at http://pubs.acs.org.

■ AUTHOR INFORMATION

Corresponding Author

*Department of Pathobiology (NC-22), Lerner Research Institute, The Cleveland Clinic Foundation, 9500 Euclid Ave., Cleveland, OH 44195. Phone: (216) 445-6950. Fax: (216) 636-0104. E-mail: stuehrd@ccf.org.

Funding

This work was supported by National Institutes of Health (NIH) Grants HL76491, GM51491, and GM97041 to D.J.S. and American Heart Association Grant 11POST650034 to L.H. Work completed in the laboratory of J.H.D. was also supported by NIH Grant GM26730.

Notes

The authors declare no competing financial interest.

■ ABBREVIATIONS

GAPDH, glyceraldehyde-3-phosphate dehydrogenase; EPR, electronic paramagnetic resonance; MCD, magnetic circular dichroism; DTT, dithiothreitol; IPTG, isopropyl thiogalactoside; LS, low-spin; HS, high-spin; 6c, six-coordinate; 5c, five-coordinate; CT, charge transfer

■ REFERENCES

(1) Nobeli, I., Favia, A. D., and Thornton, J. M. (2009) Protein promiscuity and its implications for biotechnology. *Nat. Biotechnol. 27*, 157−167.

(2) Pond, A. E., Roach, M. P., Thomas, M. R., Boxer, S. G., and Dawson, J. H. (2000) The H93G myoglobin cavity mutant as a versatile template for modeling heme proteins: Ferrous, ferric, and ferryl mixed-ligand complexes with imidazole in the cavity. *Inorg. Chem. 39*, 6061−6066.

(3) Perera, R., Sono, M., Sigman, J. A., Pfister, T. D., Lu, Y., and Dawson, J. H. (2003) Neutral thiol as a proximal ligand to ferrous

heme iron: Implications for heme proteins that lose cysteine thiolate ligation on reduction. *Proc. Natl. Acad. Sci. U.S.A. 100*, 3641−3646.
(4) Barber, R. D., Harmer, D. W., Coleman, R. A., and Clark, B. J. (2005) GAPDH as a housekeeping gene: Analysis of GAPDH mRNA expression in a panel of 72 human tissues. *Physiol. Genomics 21*, 389−395.
(5) Sirover, M. A. (2011) On the functional diversity of glyceraldehyde-3-phosphate dehydrogenase: Biochemical mechanisms and regulatory control. *Biochim. Biophys. Acta 1810*, 741−751.
(6) Sirover, M. A. (1996) Minireview. Emerging new functions of the glycolytic protein, glyceraldehyde-3-phosphate dehydrogenase, in mammalian cells. *Life Sci. 58*, 2271−2277.
(7) Ronimus, R. S., and Morgan, H. W. (2003) Distribution and phylogenies of enzymes of the Embden-Meyerhof-Parnas pathway from archaea and hyperthermophilic bacteria support a gluconeogenic origin of metabolism. *Archaea 1*, 199−221.
(8) Modun, B., Morrissey, J., and Williams, P. (2000) The staphylococcal transferrin receptor: A glycolytic enzyme with novel functions. *Trends Microbiol. 8*, 231−237.
(9) Ferdinand, W. (1964) The Isolation and Specific Activity of Rabbit-Muscle Glyceraldehyde Phosphate Dehydrogenase. *Biochem. J. 92*, 578−585.
(10) Campanale, N., Nickel, C., Daubenberger, C. A., Wehlan, D. A., Gorman, J. J., Klonis, N., Becker, K., and Tilley, L. (2003) Identification and characterization of heme-interacting proteins in the malaria parasite, *Plasmodium falciparum*. *J. Biol. Chem. 278*, 27354−27361.
(11) Li, X., Wang, X., Zhao, K., Zhou, Z., Zhao, C., Yan, R., Lin, L., Lei, T., Yin, J., Wang, R., Sun, Z., Xu, Z., Bao, J., Zhang, X., Feng, X., and Liu, S. (2003) A novel approach for identifying the heme-binding proteins from mouse tissues. *Genomics, Proteomics Bioinf. 1*, 78−86.
(12) Famin, O., and Ginsburg, H. (2003) The treatment of *Plasmodium falciparum*-infected erythrocytes with chloroquine leads to accumulation of ferriprotoporphyrin IX bound to particular parasite proteins and to the inhibition of the parasite's 6-phosphogluconate dehydrogenase. *Parasite 10*, 39−50.
(13) Omodeo Sale, F., Vanzulli, E., Caielli, S., and Taramelli, D. (2005) Regulation of human erythrocyte glyceraldehyde-3-phosphate dehydrogenase by ferriprotoporphyrin IX. *FEBS Lett. 579*, 5095−5099.
(14) Chakravarti, R., Aulak, K. S., Fox, P. L., and Stuehr, D. J. (2010) GAPDH regulates cellular heme insertion into inducible nitric oxide synthase. *Proc. Natl. Acad. Sci. U.S.A. 107*, 18004−18009.
(15) Li, T., Bonkovsky, H. L., and Guo, J. T. (2011) Structural analysis of heme proteins: Implications for design and prediction. *BMC Struct. Biol. 11*, 13.
(16) Rossmann, M. G., and Argos, P. (1978) The taxonomy of binding sites in proteins. *Mol. Cell. Biochem. 21*, 161−182.
(17) Gupta, N., and Ragsdale, S. W. (2011) Thiol-disulfide redox dependence of heme binding and heme ligand switching in nuclear hormone receptor rev-erb β. *J. Biol. Chem. 286*, 4392−4403.
(18) Ragsdale, S. W., and Yi, L. (2011) Thiol/disulfide redox switches in the regulation of heme binding to proteins. *Antioxid. Redox Signaling 14*, 1039−1047.
(19) Yi, L., Morgan, J. T., and Ragsdale, S. W. (2010) Identification of a thiol/disulfide redox switch in the human BK channel that controls its affinity for heme and CO. *J. Biol. Chem. 285*, 20117−20127.
(20) Hamza, I. (2006) Intracellular trafficking of porphyrins. *ACS Chem. Biol. 1*, 627−629.
(21) Aasa, R., Vanngard, T., and Dunford, H. B. (1975) EPR studies on compound I of horseradish peroxidase. *Biochim. Biophys. Acta 391*, 259−264.
(22) Zhang, J., and Snyder, S. H. (1992) Nitric oxide stimulates auto-ADP-ribosylation of glyceraldehyde-3-phosphate dehydrogenase. *Proc. Natl. Acad. Sci. U.S.A. 89*, 9382−9385.
(23) Brassard, J., Gottschalk, M., and Quessy, S. (2004) Cloning and purification of the *Streptococcus suis* serotype 2 glyceraldehyde-3-phosphate dehydrogenase and its involvement as an adhesin. *Vet. Microbiol. 102*, 87−94.
(24) Tong, Y., and Guo, M. (2007) Cloning and characterization of a novel periplasmic heme-transport protein from the human pathogen *Pseudomonas aeruginosa*. *J. Biol. Inorg. Chem. 12*, 735−750.
(25) Hannibal, L., Somasundaram, R., Tejero, J., Wilson, A., and Stuehr, D. J. (2011) Influence of heme-thiolate in shaping the catalytic properties of a bacterial nitric-oxide synthase. *J. Biol. Chem. 286*, 39224−39235.
(26) Kuzelova, K., Mrhalova, M., and Hrkal, Z. (1997) Kinetics of heme interaction with heme-binding proteins: The effect of heme aggregation state. *Biochim. Biophys. Acta 1336*, 497−501.
(27) Jarolim, P., Lahav, M., Liu, S. C., and Palek, J. (1990) Effect of hemoglobin oxidation products on the stability of red cell membrane skeletons and the associations of skeletal proteins: Correlation with a release of hemin. *Blood 76*, 2125−2131.
(28) Paul, K. G., Theorell, H., and Akeson, A. (1953) The molar light absorption of pyridine ferroprotoporphyrin (pyridine hemochromogen). *Acta Chem. Scand. 7*, 1284−1287.
(29) DiNello, R. K., and Dolphin, D. H. (1981) Substituted hemins as probes for structure-function relationships in horseradish peroxidase. *J. Biol. Chem. 256*, 6903−6912.
(30) Stoll, S., and Schweiger, A. (2006) EasySpin, a comprehensive software package for spectral simulation and analysis in EPR. *J. Magn. Reson. 178*, 42−55.
(31) Ambrosi, E., Capaldi, S., Bovi, M., Saccomani, G., Perduca, M., and Monaco, H. L. (2011) Structural changes in the BH3 domain of SOUL protein upon interaction with the anti-apoptotic protein Bcl-xL. *Biochem. J. 438*, 291−301.
(32) Lechardeur, D., Cesselin, B., Liebl, U., Vos, M. H., Fernandez, A., Brun, C., Gruss, A., and Gaudu, P. (2012) Discovery of an intracellular heme-binding protein, HrtR, that controls heme-efflux by the conserved HrtB HrtA transporter in Lactococcus lactis. *J. Biol. Chem. 287*, 4752−4758.
(33) Kirschner-Zilber, I., Rabizadeh, E., and Shaklai, N. (1982) The interaction of hemin and bilirubin with the human red cell membrane. *Biochim. Biophys. Acta 690*, 20−30.
(34) Rotsaert, F. A., Hallberg, B. M., de Vries, S., Moenne-Loccoz, P., Divne, C., Renganathan, V., and Gold, M. H. (2003) Biophysical and structural analysis of a novel heme B iron ligation in the flavocytochrome cellobiose dehydrogenase. *J. Biol. Chem. 278*, 33224−33231.
(35) Sook, B. R., Block, D. R., Sumithran, S., Montanez, G. E., Rodgers, K. R., Dawson, J. H., Eichenbaum, Z., and Dixon, D. W. (2008) Characterization of SiaA, a streptococcal heme-binding protein associated with a heme ABC transport system. *Biochemistry 47*, 2678−2688.
(36) Wojtowicz, H., Wojaczynski, J., Olczak, M., Kroliczewski, J., Latos-Grazynski, L., and Olczak, T. (2009) Heme environment in HmuY, the heme-binding protein of *Porphyromonas gingivalis*. *Biochem. Biophys. Res. Commun. 383*, 178−182.
(37) Yukl, E. T., Jepkorir, G., Alontaga, A. Y., Pautsch, L., Rodriguez, J. C., Rivera, M., and Moenne-Loccoz, P. (2010) Kinetic and spectroscopic studies of hemin acquisition in the hemophore HasAp from *Pseudomonas aeruginosa*. *Biochemistry 49*, 6646−6654.
(38) Izadi-Pruneyre, N., Huche, F., Lukat-Rodgers, G. S., Lecroisey, A., Gilli, R., Rodgers, K. R., Wandersman, C., and Delepelaire, P. (2006) The heme transfer from the soluble HasA hemophore to its membrane-bound receptor HasR is driven by protein-protein interaction from a high to a lower affinity binding site. *J. Biol. Chem. 281*, 25541−25550.
(39) Erales, J., Lignon, S., and Gontero, B. (2009) CP12 from *Chlamydomonas reinhardtii*, a permanent specific "chaperone-like" protein of glyceraldehyde-3-phosphate dehydrogenase. *J. Biol. Chem. 284*, 12735−12744.
(40) Sassa, S. (2004) Why heme needs to be degraded to iron, biliverdin IXα, and carbon monoxide? *Antioxid. Redox Signaling 6*, 819−824.
(41) Hargrove, M. S., Whitaker, T., Olson, J. S., Vali, R. J., and Mathews, A. J. (1997) Quaternary structure regulates hemin

dissociation from human hemoglobin. *J. Biol. Chem. 272*, 17385−17389.
(42) Winkler, W. C., Gonzalez, G., Wittenberg, J. B., Hille, R., Dakappagari, N., Jacob, A., Gonzalez, L. A., and Gilles-Gonzalez, M. A. (1996) Nonsteric factors dominate binding of nitric oxide, azide, imidazole, cyanide, and fluoride to the rhizobial heme-based oxygen sensor FixL. *Chem. Biol. 3*, 841−850.
(43) Yoon, J., Herzik, M. A., Jr., Winter, M. B., Tran, R., Olea, C., Jr., and Marletta, M. A. (2010) Structure and properties of a bis-histidyl ligated globin from *Caenorhabditis elegans*. *Biochemistry 49*, 5662−5670.
(44) Puranik, M., Weeks, C. L., Lahaye, D., Kabil, O., Taoka, S., Nielsen, S. B., Groves, J. T., Banerjee, R., and Spiro, T. G. (2006) Dynamics of carbon monoxide binding to cystathionine β-synthase. *J. Biol. Chem. 281*, 13433−13438.
(45) Couture, M., Burmester, T., Hankeln, T., and Rousseau, D. L. (2001) The heme environment of mouse neuroglobin. Evidence for the presence of two conformations of the heme pocket. *J. Biol. Chem. 276*, 36377−36382.
(46) Uno, T., Ryu, D., Tsutsumi, H., Tomisugi, Y., Ishikawa, Y., Wilkinson, A. J., Sato, H., and Hayashi, T. (2004) Residues in the distal heme pocket of neuroglobin. Implications for the multiple ligand binding steps. *J. Biol. Chem. 279*, 5886−5893.
(47) Pesce, A., Thijs, L., Nardini, M., Desmet, F., Sisinni, L., Gourlay, L., Bolli, A., Coletta, M., Van Doorslaer, S., Wan, X., Alam, M., Ascenzi, P., Moens, L., Bolognesi, M., and Dewilde, S. (2009) HisE11 and HisF8 provide bis-histidyl heme hexa-coordination in the globin domain of *Geobacter sulfurreducens* globin-coupled sensor. *J. Mol. Biol. 386*, 246−260.
(48) Desbois, A., and Lutz, M. (1992) Redox control of proton transfers in membrane b-type cytochromes: An absorption and resonance Raman study on bis(imidazole) and bis(imidazolate) model complexes of iron-protoporphyrin. *Eur. Biophys. J. 20*, 321−335.
(49) Takeuchi, F., Hori, H., Obayashi, E., Shiro, Y., and Tsubaki, M. (2004) Properties of two distinct heme centers of cytochrome b561 from bovine chromaffin vesicles studied by EPR, resonance Raman, and ascorbate reduction assay. *J. Biochem. 135*, 53−64.
(50) Lukat-Rodgers, G. S., Rodgers, K. R., Caillet-Saguy, C., Izadi-Pruneyre, N., and Lecroisey, A. (2008) Novel heme ligand displacement by CO in the soluble hemophore HasA and its proximal ligand mutants: Implications for heme uptake and release. *Biochemistry 47*, 2087−2098.
(51) Auclair, K., Huang, H. W., Moenne-Loccoz, P., and Ortiz de Montellano, P. R. (2003) Cloning and expression of a heme binding protein from the genome of *Saccharomyces cerevisiae*. *Protein Expression Purif. 28*, 340−349.
(52) Lou, B. S., Snyder, J. K., Marshall, P., Wang, J. S., Wu, G., Kulmacz, R. J., Tsai, A. L., and Wang, J. (2000) Resonance Raman studies indicate a unique heme active site in prostaglandin H synthase. *Biochemistry 39*, 12424−12434.
(53) Spiro, T. G. (1988) *Biological Applications of Raman Spectroscopy*, John Wiley & Sons, Toronto.
(54) Vogel, K. M., Kozlowski, P. M., Zgierski, M. Z., and Spiro, T. G. (2000) Role of the axial ligand in heme-CO backbonding; DFT analysis of vibrational data. *Inorg. Chim. Acta 297*, 11−17.
(55) Spiro, T. G., and Wasbotten, I. H. (2005) CO as a vibrational probe of heme protein active sites. *J. Inorg. Biochem. 99*, 34−44.
(56) Argos, P., and Mathews, F. S. (1975) The structure of ferrocytochrome b5 at 2.8 Å resolution. *J. Biol. Chem. 250*, 747−751.
(57) Babcock, G. T., Widger, W. R., Cramer, W. A., Oertling, W. A., and Metz, J. G. (1985) Axial ligands of chloroplast cytochrome b-559: Identification and requirement for a heme-cross-linked polypeptide structure. *Biochemistry 24*, 3638−3645.
(58) Dou, Y., Admiraal, S. J., Ikeda-Saito, M., Krzywda, S., Wilkinson, A. J., Li, T., Olson, J. S., Prince, R. C., Pickering, I. J., and George, G. N. (1995) Alteration of axial coordination by protein engineering in myoglobin. Bisimidazole ligation in the His64→Val/Val68→His double mutant. *J. Biol. Chem. 270*, 15993−16001.
(59) Halder, P., Trent, J. T., III, and Hargrove, M. S. (2007) Influence of the protein matrix on intramolecular histidine ligation in ferric and ferrous hexacoordinate hemoglobins. *Proteins 66*, 172−182.
(60) Miller, G. T., Zhang, B., Hardman, J. K., and Timkovich, R. (2000) Converting a c-type to a b-type cytochrome: Met61 to His61 mutant of *Pseudomonas* cytochrome c-551. *Biochemistry 39*, 9010−9017.
(61) Raphael, A. L., and Gray, H. B. (1989) Axial ligand replacement in horse heart cytochrome c by semisynthesis. *Proteins 6*, 338−340.
(62) Ishikawa, H., Nakagaki, M., Bamba, A., Uchida, T., Hori, H., O'Brian, M. R., Iwai, K., and Ishimori, K. (2011) Unusual heme binding in the bacterial iron response regulator protein: Spectral characterization of heme binding to the heme regulatory motif. *Biochemistry 50*, 1016−1022.
(63) Yang, F., Xia, X., Lei, H. Y., and Wang, E. D. (2010) Hemin binds to human cytoplasmic arginyl-tRNA synthetase and inhibits its catalytic activity. *J. Biol. Chem. 285*, 39437−39446.
(64) Seidler, N. W. (2013) Basic Biology of GAPDH. *Adv. Exp. Med. Biol. 985*, 1−36.
(65) Hargrove, M. S., Barrick, D., and Olson, J. S. (1996) The association rate constant for heme binding to globin is independent of protein structure. *Biochemistry 35*, 11293−11299.
(66) Bhakta, M. N., and Wilks, A. (2006) The mechanism of heme transfer from the cytoplasmic heme binding protein PhuS to the δ-regioselective heme oxygenase of *Pseudomonas aeruginosa*. *Biochemistry 45*, 11642−11649.
(67) Hargrove, M. S., Wilkinson, A. J., and Olson, J. S. (1996) Structural factors governing hemin dissociation from metmyoglobin. *Biochemistry 35*, 11300−11309.
(68) Bianchetti, C. M., Blouin, G. C., Bitto, E., Olson, J. S., and Phillips, G. N., Jr. (2010) The structure and NO binding properties of the nitrophorin-like heme-binding protein from *Arabidopsis thaliana* gene locus At1g79260.1. *Proteins 78*, 917−931.
(69) Miksanova, M., Igarashi, J., Minami, M., Sagami, I., Yamauchi, S., Kurokawa, H., and Shimizu, T. (2006) Characterization of heme-regulated eIF2α kinase: Roles of the N-terminal domain in the oligomeric state, heme binding, catalysis, and inhibition. *Biochemistry 45*, 9894−9905.
(70) Dage, J. L., Sun, H., and Halsall, H. B. (1998) Determination of diethylpyrocarbonate-modified amino acid residues in α1-acid glycoprotein by high-performance liquid chromatography electrospray ionization-mass spectrometry and matrix-assisted laser desorption/ionization time-of-flight-mass spectrometry. *Anal. Biochem. 257*, 176−185.
(71) Hayasaka, K., Kitanishi, K., Igarashi, J., and Shimizu, T. (2011) Heme-binding characteristics of the isolated PAS-B domain of mouse Per2, a transcriptional regulatory factor associated with circadian rhythms. *Biochim. Biophys. Acta 1814*, 326−333.
(72) Konkle, M. E., Elsenheimer, K. N., Hakala, K., Robicheaux, J. C., Weintraub, S. T., and Hunsicker-Wang, L. M. (2010) Chemical modification of the Rieske protein from *Thermus thermophilus* using diethyl pyrocarbonate modifies ligating histidine 154 and reduces the [2FE-2S] cluster. *Biochemistry 49*, 7272−7281.
(73) Tawfik, D. S. (2002) Ethoxyformylation of Histidine. In *The Protein Protocols Handbook*, 2nd ed. (Walker, J. M., Ed.) Chapter 65, pp 473−474, Springer, Dordrecht, The Netherlands.
(74) Ran, Y., Liu, M., Zhu, H., Nygaard, T. K., Brown, D. E., Fabian, M., Dooley, D. M., and Lei, B. (2010) Spectroscopic identification of heme axial ligands in HtsA that are involved in heme acquisition by *Streptococcus pyogenes*. *Biochemistry 49*, 2834−2842.
(75) Puranik, M., Nielsen, S. B., Youn, H., Hvitved, A. N., Bourassa, J. L., Case, M. A., Tengroth, C., Balakrishnan, G., Thorsteinsson, M. V., Groves, J. T., McLendon, G. L., Roberts, G. P., Olson, J. S., and Spiro, T. G. (2004) Dynamics of carbon monoxide binding to CooA. *J. Biol. Chem. 279*, 21096−21108.
(76) Moller, J. K., and Skibsted, L. H. (2004) Mechanism of nitrosylmyoglobin autoxidation: Temperature and oxygen pressure effects on the two consecutive reactions. *Chemistry 10*, 2291−2300.

(77) Pierre, J. L., Fontecave, M., and Crichton, R. R. (2002) Chemistry for an essential biological process: The reduction of ferric iron. *BioMetals 15*, 341−346.
(78) Gaspard, S., Chottard, G., Mahy, J. P., and Mansuy, D. (1996) Study of the coordination chemistry of prostaglandin G/H synthase by resonance Raman spectroscopy. *Eur. J. Biochem. 238*, 529−537.
(79) Choi, C. Y., Cerda, J. F., Chu, H. A., Babcock, G. T., and Marletta, M. A. (1999) Spectroscopic characterization of the heme-binding sites in *Plasmodium falciparum* histidine-rich protein 2. *Biochemistry 38*, 16916−16924.
(80) Dailey, T. A., Boynton, T. O., Albetel, A. N., Gerdes, S., Johnson, M. K., and Dailey, H. A. (2010) Discovery and Characterization of HemQ: An essential heme biosynthetic pathway component. *J. Biol. Chem. 285*, 25978−25986.
(81) Airola, M. V., Du, J., Dawson, J. H., and Crane, B. R. (2010) Heme binding to the mammalian circadian clock protein period 2 is nonspecific. *Biochemistry 49*, 4327−4338.
(82) Spolaore, B., De Filippis, V., and Fontana, A. (2005) Heme binding by the N-terminal fragment 1−44 of human growth hormone. *Biochemistry 44*, 16079−16089.
(83) Hrkal, Z., Vodrazka, Z., and Kalousek, I. (1974) Transfer of heme from ferrihemoglobin and ferrihemoglobin isolated chains to hemopexin. *Eur. J. Biochem. 43*, 73−78.
(84) Leclerc, E., Leclerc, L., Poyart, C., and Marden, M. C. (1993) Interaction of heme with amphiphilic peptides: Use of hemin-CN to probe the interaction of calmodulin with its target peptides. *Arch. Biochem. Biophys. 306*, 158−162.
(85) Marden, M. C., Dufour, E., Christova, P., Huang, Y., Leclerc-L'Hostis, E., and Haertle, T. (1994) Binding of heme-CO to bovine and porcine *β*-lactoglobulins. *Arch. Biochem. Biophys. 311*, 258−262.
(86) Wardell, M., Wang, Z., Ho, J. X., Robert, J., Ruker, F., Ruble, J., and Carter, D. C. (2002) The atomic structure of human methemalbumin at 1.9 Å. *Biochem. Biophys. Res. Commun. 291*, 813−819.
(87) Zhang, L., and Guarente, L. (1995) Heme binds to a short sequence that serves a regulatory function in diverse proteins. *EMBO J. 14*, 313−320.
(88) Poulos, T. L. (1996) The role of the proximal ligand in heme enzymes. *J. Biol. Inorg. Chem. 1*, 356−359.
(89) Reedy, C. J., and Gibney, B. R. (2004) Heme protein assemblies. *Chem. Rev. 104*, 617−649.
(90) Schultz, I. J., Chen, C., Paw, B. H., and Hamza, I. (2010) Iron and porphyrin trafficking in heme biogenesis. *J. Biol. Chem. 285*, 26753−26759.
(91) de Rosny, E., de Groot, A., Jullian-Binard, C., Borel, F., Suarez, C., Le Pape, L., Fontecilla-Camps, J. C., and Jouve, H. M. (2008) DHR51, the *Drosophila melanogaster* homologue of the human photoreceptor cell-specific nuclear receptor, is a thiolate heme-binding protein. *Biochemistry 47*, 13252−13260.
(92) Daltrop, O., Stevens, J. M., Higham, C. W., and Ferguson, S. J. (2002) The CcmE protein of the *c*-type cytochrome biogenesis system: unusual *in vitro* heme incorporation into apo-CcmE and transfer from holo-CcmE to apocytochrome. *Proc. Natl. Acad. Sci. U.S.A. 99*, 9703−9708.
(93) Nygaard, T. K., Blouin, G. C., Liu, M., Fukumura, M., Olson, J. S., Fabian, M., Dooley, D. M., and Lei, B. (2006) The mechanism of direct heme transfer from the streptococcal cell surface protein Shp to HtsA of the HtsABC transporter. *J. Biol. Chem. 281*, 20761−20771.
(94) Ran, Y., Zhu, H., Liu, M., Fabian, M., Olson, J. S., Aranda, R. t., Phillips, G. N., Jr., Dooley, D. M., and Lei, B. (2007) Bis-methionine ligation to heme iron in the streptococcal cell surface protein Shp facilitates rapid hemin transfer to HtsA of the HtsABC transporter. *J. Biol. Chem. 282*, 31380−31388.
(95) Owens, C. P., Du, J., Dawson, J. H., and Goulding, C. W. (2012) Characterization of heme ligation properties of Rv0203, a secreted heme binding protein involved in *Mycobacterium tuberculosis* heme uptake. *Biochemistry 51*, 1518−1531.